

Remarks on Interacting Neimark-Sacker Bifurcations

Yu. A. Kuznetsov, H.G.E. Meijer,
Mathematisch Instituut, Budapestlaan 6,
PO-Box 80010 3508 TA Utrecht, Netherlands

January 10, 2006

Abstract

We study codimension-2 bifurcations of fixed points of dissipative diffeomorphisms with a pair of complex critical eigenvalues together with either an eigenvalue -1 or another such a pair. In the previous studies only cubic normal forms were considered. However, in some cases the unfolding requires higher order terms and these are investigated here. We (re)derive the normal forms and reduce them to a single amplitude map. This map is similar to the amplitude system for the double-Hopf bifurcation for vector fields. We show how the critical normal form coefficients determine the general bifurcation picture for this amplitude map. Generic nonsymmetric perturbations of the normal forms are considered. Our case studies show a detailed picture near various bifurcation curves, which was somewhat richer than the theoretical predictions. For arbitrary maps with these bifurcations we give explicit formulas for critical normal form coefficients on center manifolds and apply them to two examples. Here we are able to demonstrate the existence of the bubble-structure, which was only observed in unfolded normal forms before.

1 Introduction

Over the past decade the analysis of local codimension 2 bifurcations of discrete-time dynamical systems generated by iterated maps (first order nonlinear difference equations) has been more or less completed. The critical cases with one- and two-dimensional center manifolds are treated in [1, 2, 3, 4]. The analysis of one of the 3-dimensional cases, namely the fold-Neimark-Sacker bifurcation, has been undertaken in [5, 6]. Here we contribute to the two remaining cases, namely a bifurcation of a fixed point with a pair of complex eigenvalues (multipliers) of modulus 1 together with either an eigenvalue -1 or another such a pair. We call them the *flip-Neimark-Sacker* (*flip-NS*) and *double Neimark-Sacker* (*NS-NS*) bifurcations, respectively. This work is not the first contribution on the topic, since these cases have also been studied in [7, 8, 9]. However those studies were concerned only with interesting but specific details, namely the quasi-periodic bifurcation of a ‘period-2’ invariant circle, which originated via a ‘doubling’ of a ‘period-1’ invariant circle, and a quasi-periodic bifurcation of the invariant circle into a 2-torus (“torification”) in the four dimensional case. These results exclude a region with so-called Chenciner bubbles where resonances occur. In some unfoldings of these cases, these tori bifurcate once more, into higher dimensional tori. In these cases, a higher-order normal form is necessary to establish stability results. Here we give a rather complete description of these bifurcations by making the right correspondence with the double Hopf bifurcation of vector fields. Moreover, we study numerically representative perturbations, which break the symmetry of the normal forms. This reveals a peculiar bifurcation structure of the bubbles. We note that such bifurcations have been found in [10, 11, 12] but not understood, and that in [13, 14] only a limited analysis is done.

The paper is organized as follows. We will (re)derive the normal forms, give the unfolding and asymptotic expressions for local and some global codim 1 bifurcations. The invariant circles may bifurcate into a 2-torus. We will analyse the birth, the dynamics and the destruction of these 2-tori in symmetric and nonsymmetric settings. For a multidimensional map exhibiting

these bifurcations we will then derive coefficients of the normal forms of the restricted map on the center manifold. This will allow us to study bifurcations of a specific map appearing in robotics, and a parametrically excited system. To facilitate the reading, all proofs are confined to a separate Appendix.

Acknowledgments

The authors would like to thank A. Vanderbauwhede for discussions related and unrelated to this research. We are also thankful to F. Verhulst and A. Steindl for help on the examples, H.W. Broer and C. Simó for suggestions on Lyapunov exponents and T. Bakri and H. Hanßmann for useful discussions.

2 Normal forms

In this section we derive the normal forms in the minimal dimensions explicitly and perform a reduction to a planar map, whose bifurcations we will study in the next section. For the bifurcations under consideration the normal forms up to and including third order may be extracted from [7, 9]. The 3-jet of such a family will be shown sufficient to distinguish several topological unfoldings. For some of them, a possible bifurcation is that of an invariant circle \mathbb{T}^1 into a \mathbb{T}^2 for the flip-NS case, (or a \mathbb{T}^2 into a \mathbb{T}^3 for the double NS). The results of the bifurcation analysis will show that it is necessary to study the 5-jet to determine the stability of the \mathbb{T}^2 (or \mathbb{T}^3). The Poincaré normal forms contain six resonant monomials of order 5; however, we will show under natural nondegeneracy conditions that for both the flip-NS and the NS-NS cases only three such terms enter the analysis.

2.1 Poincaré normal forms

Consider two maps, $F_1 : \mathbb{R}^3 \rightarrow \mathbb{R}^3$ and $F_2 : \mathbb{R}^4 \rightarrow \mathbb{R}^4$, both having a fixed point at the origin, where their linear part is given by

$$DF_1 = \begin{pmatrix} -1 & 0 & 0 \\ 0 & \cos(\phi) & -\sin(\phi) \\ 0 & \sin(\phi) & \cos(\phi) \end{pmatrix}$$

and

$$DF_2 = \begin{pmatrix} \cos(\phi_1) & -\sin(\phi_1) & 0 & 0 \\ \sin(\phi_1) & \cos(\phi_1) & 0 & 0 \\ 0 & 0 & \cos(\phi_2) & -\sin(\phi_2) \\ 0 & 0 & \sin(\phi_2) & \cos(\phi_2) \end{pmatrix}.$$

For F_1 the origin has multipliers $\lambda \in S_1 \equiv \{-1, e^{i\phi}, e^{-i\phi}\}$, while for F_2 the multipliers are $\lambda \in S_2 \equiv \{e^{i\phi_1}, e^{-i\phi_1}, e^{i\phi_2}, e^{-i\phi_2}\}$, with $0 < \phi, \phi_1, \phi_2 < \pi$.

Now we embed these maps into finite-parameter families. Since $1 \notin S_{1,2}$, we can assume without loss of generality that the origin is a fixed point for all parameter values. Thus, the Jacobian matrices evaluated at the fixed point in the origin become functions of parameters, $DF_1(\alpha)$ and $DF_2(\alpha)$. Denote the eigenvalues of $DF_1(\alpha)$ by $\lambda_1(\alpha), \lambda_2(\alpha) = \bar{\lambda}_3(\alpha)$ and those of $DF_2(\alpha)$ by $\lambda_1(\alpha) = \bar{\lambda}_3(\alpha), \lambda_2(\alpha) = \bar{\lambda}_4(\alpha)$. To place all eigenvalues of a generic parameter-dependent 3×3 or 4×4 real matrix with complex pairs on the unit circle, one needs two unfolding parameters $\alpha = (\alpha_1, \alpha_2)$. The arguments (angles) ϕ, ϕ_1, ϕ_2 then become functions of α , i.e. $\phi(\alpha), \phi_1(\alpha), \phi_2(\alpha)$. If their critical values corresponding to $\alpha = 0$ are not equal to $2\pi p/q$, $p, q \in \mathbb{N}$ and q a small integer, then they may effectively be treated as constants for $\alpha \neq 0$. Introducing more parameters we can perturb the critical angles, however, as we shall see later, there are only small regions in parameter space where effects of varying the angles are significant.

Since the critical fixed points are nonhyperbolic, nonlinear terms have to be introduced. With the aid of the normal form reduction only resonant terms will remain. It is also natural to identify \mathbb{R}^3 with $\mathbb{R} \times \mathbb{C}$ and \mathbb{R}^4 with $\mathbb{C} \times \mathbb{C}$, so that F_1 and F_2 become smooth transformations of these spaces with the critical linear parts

$$A_1 = \begin{pmatrix} -1 & 0 \\ 0 & e^{i\phi(0)} \end{pmatrix} \text{ and } A_2 = \begin{pmatrix} e^{i\phi_1(0)} & 0 \\ 0 & e^{i\phi_2(0)} \end{pmatrix},$$

respectively. The normalizing changes of variables could also be considered as smooth nonlinear transformations of $\mathbb{R} \times \mathbb{C}$ or $\mathbb{C} \times \mathbb{C}$. After these considerations we now give the parameter dependent normal forms, which will be studied in the rest of the paper.

Proposition 2.1 *Let $F_1 : \mathbb{R} \times \mathbb{C} \times \mathbb{R}^2 \rightarrow \mathbb{R} \times \mathbb{C}$ be a smooth two-parameter family of maps with $F_1(0, 0, \alpha) = 0$ and $DF_1(0) = A_1$. Moreover, let $(k\phi(0) \bmod 2\pi) \neq 0$ for $k = 1, 2, 3, 4, 5, 6, 8, 10$ and $\det\left(\frac{d(\lambda_1(\alpha), |\lambda_2(\alpha)|)}{d(\alpha_1, \alpha_2)}\right) \neq 0$. Then the family F_1 is locally smoothly conjugate to a map with the 5-jet with respect to (x, z) :*

$$NF_1 : \begin{pmatrix} x \\ z \end{pmatrix} \mapsto \begin{pmatrix} -x(1 + \mu_1) \\ z(1 + \mu_2)e^{i\phi(\mu)} \end{pmatrix} + \begin{pmatrix} x(f_{300}x^2 + f_{111}|z|^2 + f_{500}x^4 + f_{311}x^2|z|^2 + f_{122}|z|^4) \\ z(g_{210}x^2 + g_{021}|z|^2 + g_{410}x^4 + g_{221}x^2|z|^2 + g_{032}|z|^4) \end{pmatrix}, \quad (1)$$

where f_{ijk} are real and g_{ijk} complex smooth functions of $\mu = (\mu_1, \mu_2)$.

Let $F_2 : \mathbb{C}^2 \times \mathbb{R}^2 \rightarrow \mathbb{C}^2$ be a smooth two-parameter family of maps with $F_2(0, 0, \alpha) = 0$ and $DF_2(0) = A_2$. Moreover, let $(k\phi_i(0) \bmod 2\pi) \neq 0$ for $k = 1, 2, 3, 4, 5, 6$ and $i = 1, 2$ and $(\phi_1(0)/\phi_2(0)) \notin \pm\{5, 4, 3, 2, \frac{3}{2}, 1, \frac{2}{3}, \frac{1}{2}, \frac{1}{3}, \frac{1}{4}, \frac{1}{5}\}$ and $\det\left(\frac{d(|\lambda_1(\alpha)|, |\lambda_2(\alpha)|)}{d(\alpha_1, \alpha_2)}\right) \neq 0$. Then the family F_2 is locally smoothly conjugate to a map with the 5-jet with respect to (w, z) :

$$NF_2 : \begin{pmatrix} w \\ z \end{pmatrix} \mapsto \begin{pmatrix} w(1 + \mu_1)e^{i\phi_1(\mu)} \\ z(1 + \mu_2)e^{i\phi_2(\mu)} \end{pmatrix} + \begin{pmatrix} w(f_{2100}|w|^2 + f_{1011}|z|^2 + f_{3200}|w|^4 + f_{2111}|w|^2|z|^2 + f_{1022}|z|^4) \\ z(g_{1110}|w|^2 + g_{0021}|z|^2 + g_{2201}|w|^4 + g_{1121}|w|^2|z|^2 + g_{0032}|z|^4) \end{pmatrix}, \quad (2)$$

where f_{ijkl} and g_{ijkl} are smooth complex functions of $\mu = (\mu_1, \mu_2)$.

Proof. See section 8.1. □

The conditions on $\phi(0), \phi_1(0), \phi_2(0)$ imply the absence of strong resonances. In cases when the 3-jet determines the complete topological unfolding, the conditions can be relaxed to $k = 1, 2, 3, 4, 6$ for the normal form of the flip-NS bifurcation. For the normal form of the double NS bifurcation, we get $k = 1, 2, 3, 4$ and $(\phi_1(0)/\phi_2(0)) \notin \pm\{3, 2, 1, \frac{1}{2}, \frac{1}{3}\}$.

Remark 2.2 The detection of a fixed point with critical multipliers in S_1 or S_2 is a simple task supported, for example, by CONTENT[15]. Checking the transversality of the families F_1 and F_2 with respect to parameters α_1 and α_2 is more difficult, since, in general, one does not have explicit expressions for the multipliers. However, there are two functions, G_1 and G_2 , whose regularity at the origin is equivalent to the regularity required in Proposition 2.1.

For the flip-NS bifurcation, the regularity at $(X, \alpha) = (0, 0)$ of the map $G_1 : \mathbb{R}^3 \times \mathbb{R}^2 \rightarrow \mathbb{R}^3 \times \mathbb{R}^2$,

$$G_1(X, \alpha) = (F_1(X, \alpha), \det(DF_1(\alpha) + I_3), \det(DF_1(\alpha) + 1)),$$

is equivalent to the condition

$$16 \sin^2(\phi(0)) \det\left(\frac{d(\lambda_1, |\lambda_2|)}{d(\alpha_1, \alpha_2)}\right) \neq 0.$$

For the double NS bifurcation, a similar condition is more involved. We follow [16, Chapter 5.5]. The 6×6 -matrix $M(\alpha) = DF_2(\alpha) \odot DF_2(\alpha) - I_6$, where \odot denotes the bialternate product, has rank defect two at $\alpha = 0$. Choose $B, C \in \mathbb{R}^{n \times 2}, D \in \mathbb{R}^{2 \times 2}$ such that $\begin{pmatrix} M(\alpha) & B \\ C^T & D \end{pmatrix}$ is nonsingular for small α , and define $G(\alpha) \in \mathbb{R}^{2 \times 2}$ as the solution of the following equation

$$\begin{pmatrix} M(\alpha) & B \\ C^T & D \end{pmatrix} \begin{pmatrix} Q \\ G(\alpha) \end{pmatrix} = \begin{pmatrix} 0 \\ I_2 \end{pmatrix}.$$

The double Neimark-Sacker bifurcation is then characterized by $G(0)$ being the null-matrix. Since only two of the four elements are independent, we can choose any two of them, say $g_{11}(\alpha)$ and $g_{22}(\alpha)$. Then the regularity at $(X, \alpha) = (0, 0)$ of the map $G_2 : \mathbb{R}^5 \rightarrow \mathbb{R}^5$,

$$G_2(X, \alpha) = (F_2(X, \alpha), g_{11}(\alpha), g_{22}(X, \alpha)),$$

can be expressed as

$$16(\cos(\phi_1(0)) - 1)(\cos(\phi_2(0)) - 1) \det \left(\frac{d(|\lambda_1(\alpha)|, |\lambda_2(\alpha)|)}{d(\alpha_1, \alpha_2)} \right) \neq 0.$$

Therefore, the transversality can be checked in the original real coordinates as the regularity of the map G_1 or G_2 at the origin. We refer to the Appendix for some computations related to this Remark. A method to verify the transversality presented in [11] involves the computation of eigenvectors and is more laborious.

2.2 Reduction to an amplitude map

Both truncated normal forms (1) and (2) are equivariant under rotations and reflections. If we factor these symmetries out and truncate higher-order terms, then both maps are reduced to a single map:

$$H_\mu : \begin{pmatrix} x \\ y \end{pmatrix} \mapsto \begin{pmatrix} (1 + \mu_1)x + a_{11}x^3 + a_{12}xy^2 + h_{50}x^5 + h_{32}x^3y^2 + h_{14}xy^4 \\ (1 + \mu_2)y + a_{21}x^2y + a_{22}y^3 + h_{41}x^4y + h_{23}x^2y^3 + h_{05}y^5 \end{pmatrix}. \quad (3)$$

As before, we suppress the parameter dependence of the coefficients a_{ij} . This affects the expressions for the bifurcation curves of the Neimark-Sacker and heteroclinic bifurcations in Proposition 3.1, but not the stability of the invariant circle, see also Remark 3.2 in Section 3. In that sense the suppression is harmless.

For the flip-NS bifurcation we introduce cylindrical coordinates (x, r, ψ) , where $z = re^{i\psi}$. Then map (1) becomes

$$\begin{pmatrix} x \\ r \\ \psi \end{pmatrix} \mapsto \begin{pmatrix} x \left(-(1 + \mu_1) + a_{11}x^2 + a_{12}r^2 + h_{50}x^4 + h_{32}x^2r^2 + h_{14}r^4 \right) \\ r \left(1 + \mu_2 + a_{21}x^2 + a_{22}r^2 + h_{41}x^4 + h_{23}x^2r^2 + h_{05}r^4 \right) \\ \psi + \phi(\mu) + \Im(e^{-i\phi(\mu)} g_{021})r^2 + \Im(e^{-i\phi(\mu)} g_{210})x^2 \end{pmatrix} + \mathcal{O} \begin{pmatrix} 0 \\ \|(x, r)\|^6 \\ \|(x, r)\|^3 \end{pmatrix}. \quad (4)$$

Remark that the first two components of (4) are independent of ψ . Ignoring the ψ -equation and the higher-order terms for the moment, we identify (1) with (3) by composing (4) with the reflection $R = \begin{pmatrix} -1 & 0 \\ 0 & 1 \end{pmatrix}$. The correspondence is then given by the formulas a_{ij} and h_{ij} as

$$\begin{pmatrix} a_{11} & a_{12} \\ a_{21} & a_{22} \end{pmatrix} = \begin{pmatrix} -f_{300} & -f_{111} \\ \Re(e^{-i\phi} g_{210}) & \Re(e^{-i\phi} g_{021}) \end{pmatrix}$$

and

$$\begin{aligned} h_{50} &= f_{500}, & h_{41} &= \Re(e^{-i\phi} g_{410}) + \frac{1}{2} \Im(e^{-i\phi} g_{210})^2, \\ h_{32} &= f_{311}, & h_{23} &= \Re(e^{-i\phi} g_{311}) + \Im(e^{-i\phi} g_{210}) \Im(e^{-i\phi} g_{021}), \\ h_{14} &= f_{122}, & h_{05} &= \Re(e^{-i\phi} g_{032}) + \frac{1}{2} \Im(e^{-i\phi} g_{021})^2. \end{aligned}$$

For the NS-NS bifurcation we introduce, as above, polar coordinates $(r_1, r_2, \psi_1, \psi_2)$, where $(w, z) = (r_1 e^{\psi_1}, r_2 e^{\psi_2})$. Then (2) transforms into

$$\begin{aligned} \begin{pmatrix} r_1 \\ r_2 \\ \psi_1 \\ \psi_2 \end{pmatrix} &\mapsto \begin{pmatrix} r_1(1 + \mu_1 + a_{11}r_1^2 + a_{12}r_2^2 + h_{50}r_1^4 + h_{32}r_1^2r_2^2 + h_{14}r_2^4) \\ r_2(1 + \mu_2 + a_{21}r_1^2 + a_{22}r_2^2 + h_{41}r_1^4 + h_{23}r_1^2r_2^2 + h_{05}r_2^4) \\ \psi_1 + \phi_1(\mu) + \Im(e^{-i\phi_1(\mu)} g_{2100})r_1^2 + \Im(e^{-i\phi_1(\mu)} g_{1011})r_2^2 \\ \psi_2 + \phi_2(\mu) + \Im(e^{-i\phi_2(\mu)} g_{1110})r_1^2 + \Im(e^{-i\phi_2(\mu)} g_{0021})r_2^2 \end{pmatrix} \\ &+ \mathcal{O} \left(\begin{pmatrix} \|(r_1, r_2)\|^6 \\ \|(r_1, r_2)\|^6 \\ \|(r_1, r_2)\|^3 \\ \|(r_1, r_2)\|^3 \end{pmatrix} \right), \end{aligned} \quad (5)$$

where the coefficients are given by

$$\begin{pmatrix} a_{11} & a_{12} \\ a_{21} & a_{22} \end{pmatrix} = \begin{pmatrix} \Re(e^{-i\phi_1} f_{2100}) & \Re(e^{-i\phi_1} f_{1011}) \\ \Re(e^{-i\phi_2} g_{1110}) & \Re(e^{-i\phi_2} g_{0021}) \end{pmatrix}$$

and

$$\begin{aligned} h_{50} &= \Re(e^{-i\phi_1} f_{4100}) + \frac{1}{2} \Im(e^{-i\phi_1} f_{2100})^2, \\ h_{41} &= \Re(e^{-i\phi_2} g_{2210}) + \frac{1}{2} \Im(e^{-i\phi_2} g_{1110})^2, \\ h_{32} &= \Re(e^{-i\phi_1} f_{2111}) + \Im(e^{-i\phi_1} f_{2100}) \Im(e^{-i\phi_1} f_{1011}), \\ h_{23} &= \Re(e^{-i\phi_2} g_{1121}) + \Im(e^{-i\phi_2} g_{1110}) \Im(e^{-i\phi_2} g_{0021}), \\ h_{14} &= \Re(e^{-i\phi_1} f_{1022}) + \frac{1}{2} \Im(e^{-i\phi_1} f_{1011})^2, \\ h_{05} &= \Re(e^{-i\phi_2} g_{0032}) + \frac{1}{2} \Im(e^{-i\phi_2} g_{0021})^2. \end{aligned}$$

As in the flip-NS case, the first two components are independent of ψ_1 and ψ_2 , and we obtain the identification of (2) with (3), if the higher order terms are truncated.

2.3 Hypernormalization

We see that four cubic terms remain in the amplitude map. We can use these cubic coefficients of the resonant monomials to remove some of the fifth-order terms. In fact the following statement holds.

Proposition 2.3 *If $a_{11}a_{22} \neq 0$ and $a_{12}a_{21}(a_{12} - a_{22}) \neq 0$, then the family H_μ given by (3) is smoothly conjugated to a family with the 5-jet*

$$\begin{pmatrix} x \\ y \end{pmatrix} \mapsto F_\mu(x, y) = \begin{pmatrix} x(1 + \mu_1) + s_1 x^3 + s_2 \theta x y^2 + c_1 x^5 \\ y(1 + \mu_2) + s_1 \delta x^2 y + s_2 y^3 + c_4 x^4 y + c_6 y^5 \end{pmatrix}, \quad (6)$$

where $s_1 = \text{sign } a_{11}$, $s_2 = \text{sign } a_{22}$,

$$\theta = \frac{a_{12}}{a_{22}}, \quad \delta = \frac{a_{21}}{a_{11}}, \quad c_1 = \frac{h_{50}}{(a_{11})^2}, \quad c_6 = \frac{h_{05}}{(a_{22})^2}$$

and

$$c_4 = \frac{h_{41}}{(a_{11})^2} + \frac{a_{21}}{(a_{11})^2} \left(\frac{h_{32}}{a_{12}} - \frac{h_{14}(a_{11} - a_{21})}{a_{12}(a_{12} - a_{22})} - \frac{h_{23}(a_{11} - a_{21})}{a_{21}(a_{12} - a_{22})} \right).$$

Proof. See Section 8.1. □

3 Bifurcation Analysis of Symmetric Normal Forms

3.1 Bifurcations of the hypernormalized amplitude map

In this section we study bifurcations of the map (6). We recall that this map corresponds to the truncated normal forms (1) and (2). As mentioned before, it appears in other applications involving symmetry-breaking. First, we study fixed points of (6) and their stability. Then we consider the correspondence between (6) and the full maps (1) and (2). Due to the symmetries it is enough to consider the positive quadrant in the (x, y) -plane.

Proposition 3.1 *Suppose the coefficients of the map (6) satisfy the following non-degeneracy conditions*

$$(D.1) \quad s_1 s_2 \theta \delta \neq 0.$$

$$(D.2) \quad \delta \theta - 1 \neq 0.$$

$$(D.3) \quad \theta, \delta \neq 1.$$

(D.4) $L_{NS} = s_1 \left(\frac{12(2\delta\theta - \delta - \theta)}{\theta(\theta - 1)} + c_1 \frac{8(2\delta\theta - \delta - 1)}{(\theta - 1)(\delta\theta - 1)} - c_4 \frac{8}{(\delta\theta - 1)} + c_6 \frac{8\delta(2\delta\theta - \theta - 1)}{\theta(\theta - 1)(\delta\theta - 1)} \right) \neq 0$. Then, for sufficiently small (μ_1, μ_2) map (6) exhibits the following bifurcations.

- The trivial fixed point exhibits a pitchfork bifurcation at $T_1 = \{\mu \in \mathbb{R}^2 : \mu_1 = 0\}$. The semitrivial fixed point $(x, y) = (\sqrt{-s_1\mu_1}, 0)$ is stable if $s_1 < 0$ and $\mu_2 - s_1\delta\mu_1 < 0$ and totally unstable if the inequality signs are reversed. Otherwise the fixed point is a saddle.
- The trivial fixed point exhibits another a pitchfork bifurcation at $T_2 = \{\mu \in \mathbb{R}^2 : \mu_2 = 0\}$. The semitrivial fixed point $(x, y) = (0, \sqrt{-s_2\mu_2})$ is stable if $s_2 < 0$ and $\mu_1 - s_2\theta\mu_2 < 0$ and totally unstable if the inequality signs are reversed. Otherwise the fixed point is a saddle.
- If both $\rho_1^2 = \frac{(\mu_1 - \theta\mu_2)}{s_1(\delta\theta - 1)} > 0$ and $\rho_2^2 = \frac{(\mu_2 - \delta\mu_1)}{s_2(\delta\theta - 1)} > 0$ hold, then there is a nontrivial fixed point $(x, r) = (\rho_1, \rho_2) + \mathcal{O}(|\mu|^2)$. The fixed point is stable if $s_1 s_2 (\delta\theta - 1) < 0$ and $(s_1 \rho_1^2 + s_2 \rho_2^2) < 0$. It is unstable if both inequality signs are reversed.

The semitrivial fixed points on the x - and y -axes undergo secondary pitchfork bifurcations at $T_3 = \{\mu \in \mathbb{R}^2 : \mu_1 = \theta\mu_2\}$ when $\rho_2 > 0$, or at $T_4 = \{\mu \in \mathbb{R}^2 : \mu_2 = \delta\mu_1\}$ when $\rho_1 > 0$.

- If $s_2 = -s_1$ and $\delta\theta > 1$, then the nontrivial fixed point exhibits a Neimark-Sacker bifurcation. This happens along the curve $NS = \{\mu \in \mathbb{R}^2 : \mu_2 = \mu_{2,NS}(\mu_1)\}$, where

$$\mu_{2,NS} = -\frac{\delta-1}{\theta-1}\mu_1 + \left(\frac{2(\delta\theta-1)^2 + (2\delta\theta-\delta-1)c_1 - (\theta-1)c_4 + (2\delta\theta-\theta-1)c_6}{(\theta-1)^3} \right) \mu_1^2 + \mathcal{O}(\mu_1^3),$$

for $\mu_1(\theta - 1)s_1 > 0$. The bifurcating closed invariant curve is stable if $\mu_1 L_{NS} < 0$ and unstable if $\mu_1 L_{NS} > 0$.

- If $s_2 = -s_1$ and $\delta\theta > 1$, and $\theta < 0$, then stable and unstable invariant manifolds of the semitrivial fixed points are tangent along two exponentially close bifurcation curves $HET_{1,2}$, whose quadratic approximation is given by

$$\begin{aligned} \mu_{2,HET} = & -\frac{\delta-1}{\theta-1}\mu_1 + \left(\frac{(\delta\theta-1)^2}{2(\theta-1)^3} - \frac{\delta(2\delta\theta-\delta-1)}{(2\delta\theta-\theta-\delta)(\theta-1)}c_1 + \frac{\delta}{(2\delta\theta-\theta-\delta)}c_4 \right. \\ & \left. - \frac{\theta(2\delta\theta-\theta-1)(\delta-1)^2}{(2\delta\theta-\theta-\delta)(\theta-1)^3}c_6 \right) \mu_1^2 + \mathcal{O}(\mu_1^3). \end{aligned}$$

Proof. See section 8.2. □

Remark 3.2 Suppose that the heteroclinic tangencies occur. Then we have

$$\mu_{2,NS} - \mu_{2,HET} = \frac{\theta(\delta\theta - 1)^2}{8(\theta - 1)^2(2\delta\theta - \theta - \delta)} \mu_1^2 s_1 L_{NS} + \mathcal{O}(\mu_1^3).$$

Therefore, the quadratic approximations of these curves do not coincide under the imposed non-degeneracy conditions. If we include the parameter dependence of the cubic coefficients, both $\mu_{2,NS}$ and $\mu_{2,HET}$ are affected in the same manner. Their difference is still being proportional to $\mu_1^2 L_{NS}$.

Remark 3.3 If $s_1 s_2 < 0$, $\delta\theta > 1$ and $\theta > 0$ then the invariant circle of map (6), blows up and disappears through the collision with a fixed boundary of the phase plane.

Remark 3.4 The conditions on and signs of the coefficients in the proposition lead to several different unfoldings. We may assume that $\delta \leq \theta$, otherwise we can interchange x and y . We cannot scale time, but since we are working with diffeomorphisms, we can invert the map. So if $s_1 s_2 < 0$, we may assume $\mu_1 L_{NS} < 0$ and there are six different unfoldings. If $s_1 s_2 > 0$, there are five different unfoldings. We used the same notation as in [2] and the reader can refer to that text for the bifurcation diagrams.

3.2 Bifurcations of NF_1 and NF_2

In section 2.2, we have reduced the normal forms to a planar map by factoring out the \mathbb{Z}_2 - and \mathbb{S}_1 -symmetries. In order to study bifurcations of invariant objects of maps (1) and (2) we must restore these symmetries. Although in an arbitrary map with one of these bifurcations these symmetries are usually broken, the analysis of the truncated normal forms (1) and (2) still provides a skeleton of the full dynamical catalog.

3.2.1 Symmetric flip-NS

For the flip-NS bifurcation we have a reflection and rotations. The statements of Proposition 3.1 can now be interpreted for the symmetric normal form (1) as follows, see also Figure 1.

- The bifurcation at T_1 is the usual flip bifurcation. The origin changes stability in the x -direction and a period-2 orbit (dis)appears if μ_1 crosses zero.
- The bifurcation at T_2 is the usual Neimark-Sacker bifurcation. The origin changes stability in the z -direction and a closed invariant curve (dis)appears if μ_2 crosses zero.
- At the bifurcation curve T_3 we encounter a quasi-periodic doubling bifurcation, which we will denote by CD . Here a closed invariant curve consisting of one piece changes stability in the x -direction, which is accompanied by the creation or destruction of the doubled invariant curve. Below we will be more precise about what happens.
- At the bifurcation curve T_4 the period-2 cycle changes stability and a doubled invariant curve consisting of two disjoint closed curves is created or destroyed via another Neimark-Sacker bifurcation.
- If the nontrivial fixed point of (6) undergoes the Neimark-Sacker bifurcation, then from the doubled invariant curve a 2-torus \mathbb{T}^2 bifurcates, which also consists of two disjoint sets. This is also a quasi-periodic Hopf bifurcation. Below it will be denoted by CN .
- The \mathbb{T}^2 may be destroyed in a heteroclinic bifurcation or by a boundary bifurcation.

3.2.2 Symmetric double Neimark-Sacker

The double NS normal form has two rotational symmetries. The statements of Proposition 3.1 can now be interpreted as follows.

- The bifurcations at T_1 and T_2 correspond to the birth or destruction of closed invariant curves via the standard Neimark-Sacker bifurcations.

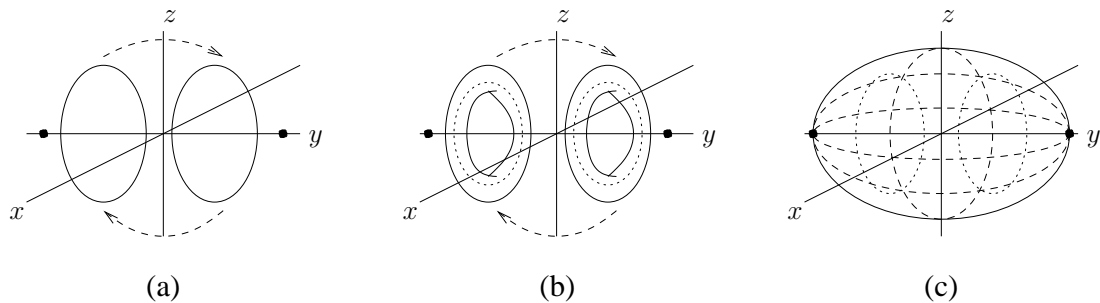


Figure 1: Sketches of phase portraits which are specific for the flip–Neimark–Sacker bifurcation. The dots represent the period-2 fixed point, which may be present or not. In (a) the doubled invariant curve is stable, in (b) and (c) it is unstable(dotted). In (b) the doubled invariant curve is surrounded by a 2-torus. In (c) the 2-torus has merged with a heteroclinic structure of the manifolds of the period-2 fixed point and the invariant curve. The doubled invariant curve exists inside.

- A bifurcation at T_3 or T_4 creates or annihilates an invariant 2-torus \mathbb{T}^2 surrounding a closed invariant curve, this is denoted as above by CN .
- The \mathbb{T}^2 may change stability such that a \mathbb{T}^3 appears, it will be labeled by TT .
- The \mathbb{T}^3 may disappear either through a heteroclinic bifurcation, where the stable and unstable manifolds of both closed invariant curves are connected, or by a collision with a fixed boundary.

4 Breaking the Symmetries

In this section we return to generic maps. In general, the higher order terms are not symmetric under the action of \mathbb{Z}_2 and \mathbb{S}_1 . In [17, 18, 19, 20, 7, 8, 9] the question of persistence of the invariant curves and tori under general dissipative perturbations was considered. The curve doubling and curve torification was subject of [7, 8, 9]. Then in [17] this is done in general for vector fields, but it can be done analogously for diffeomorphisms. These works show that there is a set of positive measure in the (μ_1, μ_2) -plane, where the bifurcation path, in general not a straight line, has a “good” bifurcation sequence. Positive measure means that it occurs with high probability and “good” means the doubling of the invariant curve or its torification without any extra dynamical phenomena. These paths avoid resonance holes and along them the reduction of the original map to the planar map is valid.

In the resonance holes, the bifurcation scenario is different. This question was first considered by Chenciner in [20]. Near the curves CD , CN , and TT we may encounter resonances on the invariant tori, and these resonance bubbles have to be avoided by a “good” path (see Figure 2 for the flip-NS case). Typically, there is a Diophantine condition which decides how large these bubbles are in parameter space.

The bifurcations of fixed points and period-2 cycles have been characterized completely by Proposition 3.1. More interesting are bifurcations of invariant curves and tori. Here we will present numerical studies in the most interesting cases, namely where a torus disappears via a heteroclinic bifurcation. Note that a boundary bifurcation, where the torus moves out of a fixed domain, may be seen as an artifact of the analysis, since in all real applications a specific mechanism destroying the torus will be visible. Phase-locking and asymmetry appear if we include the dynamics of the angles ψ in maps (4) and (5), as well as higher-order nonsymmetric terms. Thus we may encounter resonances on the invariant tori and not follow any “good” bifurcation path. Thus, in a generic nonsymmetric family complicated bifurcation sets exist near the curves CD and CN for

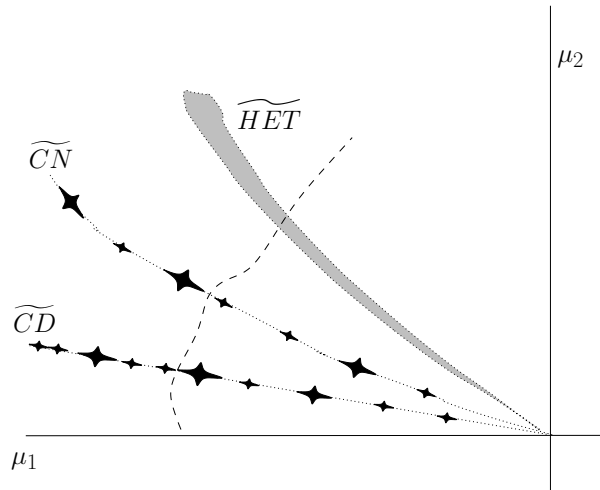


Figure 2: A sketch of the (μ_1, μ_2) -plane near a generic flip-NS bifurcation with the resonance bubbles (black diamonds) in the sets \widetilde{CD} and \widetilde{CN} . The bubbles have to be avoided by a “good” bifurcation path, like the dashed one, but are relatively small. In the region denoted by \widetilde{HET} the dynamics is complicated by heteroclinic orbits.

the flip-NS bifurcation and near the curves CN and TT for the NS-NS bifurcation, respectively, hereafter denoted by a tilde.

In [21] a theoretical framework for invariant circles with phase-locking has been developed, claimed to be representative by the authors. In our numerical case study this provides indeed a skeleton of the bifurcation scenarios. It involves coexistence of attractors and global bifurcations. However, the role of twist(imaginary parts in (7))-terms is subtle in that they lead to a codim 3 bifurcation. So the theoretical framework in [21] for the gaps describes only a part of the possibilities.

For a global overview of the dynamical inventory a two-parameter study is rather sufficient. However, near the curves CD, CN , and TT a study of three- and four-parameter unfoldings in the spirit of [22], where it was first suggested to consider the argument of the multipliers near the Neimark-Sacker bifurcation as an additional unfolding parameter, is necessary.

In our presentation we find the different bifurcation scenarios, the quasi-periodic and the periodic, next to each other. As the precise bifurcation picture depends on the higher order terms, a model map gives only a representative (not universal) picture.

4.1 Nonsymmetric flip-NS: A case study.

Let us first motivate the selection of the perturbation terms. The rotational symmetry was introduced by the normal form computations and assuming a rigid rotation in ϕ . Now we will include the dynamics of the ψ -variable in our study. Moreover we consider the situation close to a relatively low resonance, where the bifurcation structure is most pronounced. The lowest order resonance, which is permitted by the bifurcation analysis in Proposition 3.1 is the 1:7 resonance. This motivates the introduction of a third parameter μ_3 to control the detuning of the rotation and the addition of the term $\varepsilon_1 \bar{z}^{q-1}$ with $q = 7$ and ε_1 a fixed number to the second component of (1). The resulting map is still equivariant under the transformation $x \mapsto -x$. To distort this reflection symmetry, we also add the term $\varepsilon_2 x^6$ to the first component of the map. Now the symmetries are broken, but the planes $x = 0$ and $z = 0$ are still invariant. A final perturbation proportional to ε_3 is, therefore, introduced to eliminate this invariance as well. The coefficients are chosen small

such that the invariant objects under study are relatively large. Our model map is now given by

$$\begin{aligned}
F_1 : \begin{pmatrix} x \\ z \end{pmatrix} &\mapsto \begin{pmatrix} -x(1 + \mu_1) \\ z(1 + \mu_2)e^{i\mu_3} \end{pmatrix} \\
&+ \begin{pmatrix} x(f_{300}x^2 + f_{111}|z|^2 + f_{500}x^4 + f_{311}x^2|z|^2 + f_{122}|z|^4) \\ ze^{i\mu_3}(\hat{g}_{210}x^2 + \hat{g}_{021}|z|^2 + \hat{g}_{410}x^4 + \hat{g}_{221}x^2|z|^2 + \hat{g}_{032}|z|^4) \end{pmatrix} \\
&+ \begin{pmatrix} \varepsilon_2 x^6 \\ \varepsilon_1 \bar{z}^6 \end{pmatrix} + \varepsilon_3 \begin{pmatrix} (\Re(z))^6 + \Im(z)^6 \\ (x^6 + \Im(z)^6) + i(x^6 + \Re(z)^6) \end{pmatrix}.
\end{aligned} \tag{7}$$

One could take the 7th iterate of (7) and study the tongue of the period 7 cycle. Then for parameter values near the expected doubling of the single closed invariant curve one may divide out the dynamics in the r -variable in (4) to restrict the map NF_1 to a local cylinder. For such a map the effects of the lowest order perturbation terms are studied in [21]. The theoretical picture shows a richness of bifurcations involving several codim 2 bifurcations of fixed points and/or invariant curves leading to global bifurcation phenomena. The local bifurcations were understood in [21], while global ones were not treated. We may also refer to [23, 24] for a similar setting for vector fields. As the resulting formulas would be too lengthy and thus without insight, we do not take that approach here, but continue with numerical results obtained with CONTENT[15] and SDDS[25].

First we choose the coefficients, see Table 1. The cubic coefficients are such that the unfolding involves the CD - and CN -bifurcations. Then the fifth-order coefficients can be chosen such that the 2-torus is stable. The perturbation terms are arbitrarily fixed, $\varepsilon_1 = 0.5$ is larger than $\varepsilon_2 = \varepsilon_3 = 0.05$ since we want the phase-locking to be visible.

$f_{300} = -0.1$	$f_{500} = -0.5$	$\hat{g}_{410} = -0.00125$
$f_{111} = 0.3$	$f_{311} = 0$	$\hat{g}_{221} = -0.00075$
$\hat{g}_{210} = -0.25 + 0.05i$	$f_{122} = 0$	$\hat{g}_{032} = -0.0001125 - 0.025i$
$\hat{g}_{021} = -0.1 - 0.015i$		

Table 1: Numerical values of the coefficients of map (7)

We will start our numerical studies by constructing a bifurcation diagram in the two amplitude parameters (μ_1, μ_2) . We fix arbitrarily $\mu_3 = 0.9411$ and compute the Lyapunov exponents to find bifurcations of attractors as is done in [26]. The Lyapunov exponents are color-coded according to Table 2. We note that Lyapunov exponents are not a reliable tool when we are investigating a 2-torus. The second exponent converges very slowly. Thus in this case we also analyzed the frequencies as in [27] and implemented in [25]. If there were two relevant frequencies we made a continued fraction expansion of the frequency ratio. If the ratio was close to a rational number p/q with $q < 43$, this corresponded to an invariant curve on the 2-torus.

Take μ_1 negative and small, then for μ_2 small and positive we have a single stable closed invariant curve of node type (color: cyan). Increasing μ_2 we notice a few blue dots where two of its exponents become equal, however, this is not a bifurcation. Going further we see a pink stripe

Lyapunov exponents	Color	Dynamical object
$\lambda_1 > \lambda_2 \geq 0 > \lambda_3$	red	strange attractor
$\lambda_1 = \lambda_2 = 0 > \lambda_3$	magenta	invariant 2-torus
$\lambda_1 = 0 > \lambda_2 = \lambda_3$	blue	invariant circle of focus type
$\lambda_1 = 0 > \lambda_2 > \lambda_3$	cyan	invariant circle of node type
$0 > \lambda_1 \geq \lambda_2 \geq \lambda_3$	green	fixed point

Table 2: Color coding for Lyapunov exponents

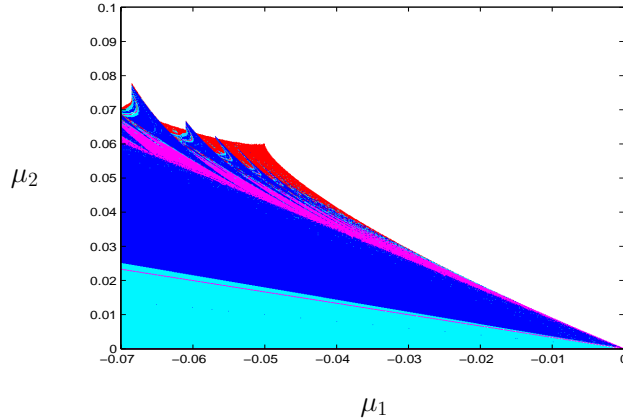


Figure 3: Bifurcation diagram in the (μ_1, μ_2) -plane near a heteroclinic connection with fixed $\mu_3 = 0.9411$

where the \widetilde{CD} bifurcation set is present. Locally, the dynamics occurs on a cylinder, which is why we code this by the same color as the 2-torus. The doubled invariant curve is initially of node type, but becomes of focus type quickly, when we get to the blue region. This doubled invariant curve bifurcates into a 2-torus via the \widetilde{CN} -transition. In the upper part of Figure 3, stripes of blue are visible, corresponding to the resonant dynamics on the 2-torus. Increasing μ_2 we cross the heteroclinic wedge encountering attractors of high period and chaos (red), and then no attractor is found anymore. The diagram in Figure 3 should be compared with the sketch given in Figure 2.

Next we fix the 2-parameter plane $\mu_1 = -.04$ in the three-dimensional parameter space, which intersects the bifurcation set in such a way that we encounter all interesting dynamics. The (μ_2, μ_3) -plane cuts the bubbles of the fractal-like bifurcation sets \widetilde{CD} and \widetilde{CN} . We present the diagrams with bifurcations of fixed points/cycles and the Lyapunov exponents next to each other, since they provide complementary information.

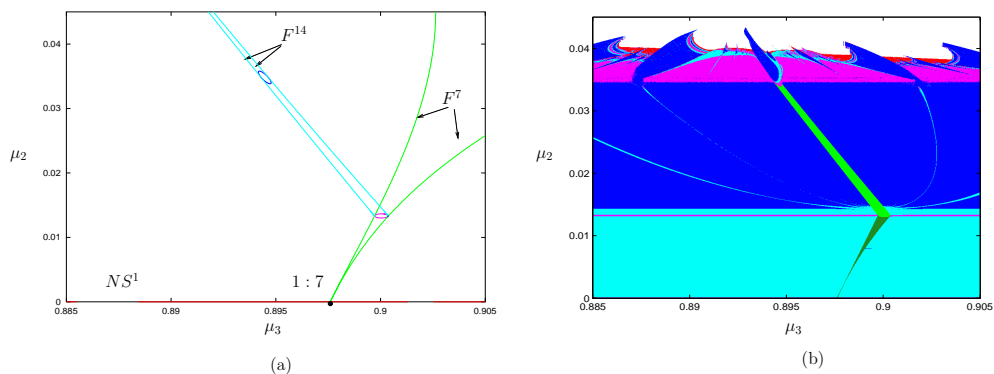


Figure 4: Bifurcation diagram for the flip-NS bifurcation. F^n and NS^n denote fold and Neimark-Sacker bifurcation of the period- n cycle, respectively. The pink circle is a period-doubling bifurcation of period-7 cycles. The dark blue circle is a Neimark-Sacker bifurcation of period-14 cycles. See enlargements in Figures 5 and 6.

Let us start with Figure 4(a), since the local bifurcation analysis guides us through the figures with the Lyapunov exponents. Actually, it produces key subsets of the whole fractal bifurcation

set. Starting at the NS^1 -curve, we find a 1:7 resonance tongue. By continuation of the tongue boundaries F^7 we arrive at the \widetilde{CD} -set, where we encounter two fold-flip points, see also Figure 5. They are of different type, where one of them involves a Neimark-Sacker, NS^{14} , and heteroclinic bifurcations, not displayed. The period doubling curve is composed of two circle segments. On both segments there is a degenerate flip bifurcation, where a fold curve of period-14 cycles is rooted. On one of the fold curves there is a 1:1-resonance, where the Neimark-Sacker bifurcation curve of period-14 cycles ends. For $\hat{g}_{210} = -0.25 - 0.06i$ we found that both degenerate flip points occurred on the upper-half of the period-doubling circle. Then on both fold-curves of the period-14 cycle a resonance 1:1 occurred.

In fact, the period-14 cycles correspond to a resonance on the doubled invariant curve. Following these fold curves, we then arrive at the \widetilde{CN} -boundary, resulting in two fold-Neimark-Sacker points. On the Neimark-Sacker curve of period-14 cycles there are two Chenciner points. Thus, the birth of the doubled torus is associated with the appearance of period-14 saddle and node cycles on the torus. The fold curves of period 14 terminate on the curve NS^2 for $\mu_2 \approx 0.1381$, which is not displayed. Somewhere in between heteroclinic bifurcations occur, which are also not visible here.

Now we turn to Figure 4(b) where the sequence of bifurcations of the invariant tori for increasing μ_2 is the same. On the invariant tori we also have resonant dynamics. We can compare this with Figure 4(a), where bifurcations of fixed points and cycles are displayed. In the green regions we have attracting cycles of period 7 and 14 on the invariant curves. The motivation for this parameter plane becomes apparent when we come to the region where the 2-torus exists. On the 2-torus, there is resonant dynamics resulting in circle attractors. These circle attractors undergo period-doubling bifurcations resulting in chaotic attractors near the heteroclinic bifurcations.

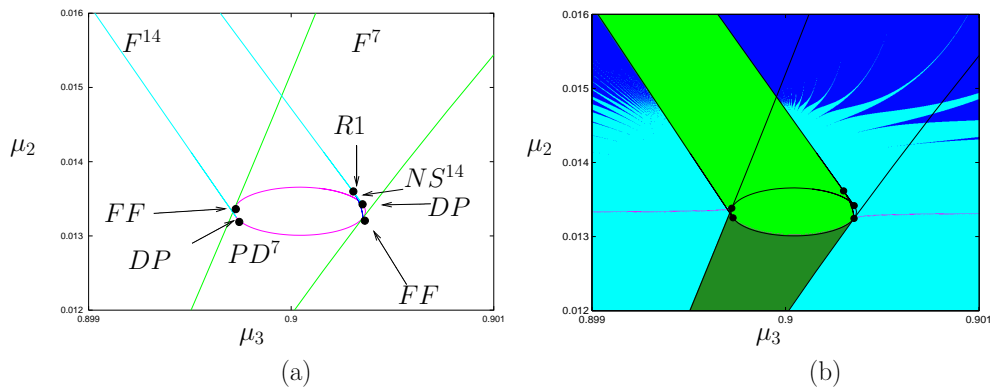


Figure 5: A subset of the bifurcation diagram near the \widetilde{CD} -boundary. NS^n denotes Neimark-Sacker bifurcation of the period- n cycles; other codim 1 curves are labeled as in Figure 4. The codim 2 points are marked FF =fold-flip, DP =degenerate flip, $R1 = 1:1$ resonance.

Let us now analyze the bubbles in more detail. We start with the case, where the phase-locking of period 7 interacts with the \widetilde{CD} bifurcation set, see Figures 5(a) and 5(b). At the bottom, we start with a single closed invariant curve of node type, either with or without phase-locking. Without phase-locking the doubling of the curve happens in the smooth quasi-periodic manner. The dynamics on a cylinder is visible as a pink stripe where two Lyapunov exponents are almost zero. Following the phase-locking, however the doubled curve exists only when we have crossed the circle of period-doubling of period 7 completely and are not near the $R1$ -point. Further up the transition of the doubled curve from node to focus type is clearly visible. The stripes where the doubled curve is of node type go up all the way, see Figure 4(b). These give rise to resonances which complicate the diagram near the \widetilde{CN} -boundary. Now the resonance of period 14 on the doubled curve has appeared and we may follow it until it disappears, i.e., at the NS^2 -bifurcation. Before that there is another bubble, which we now examine.

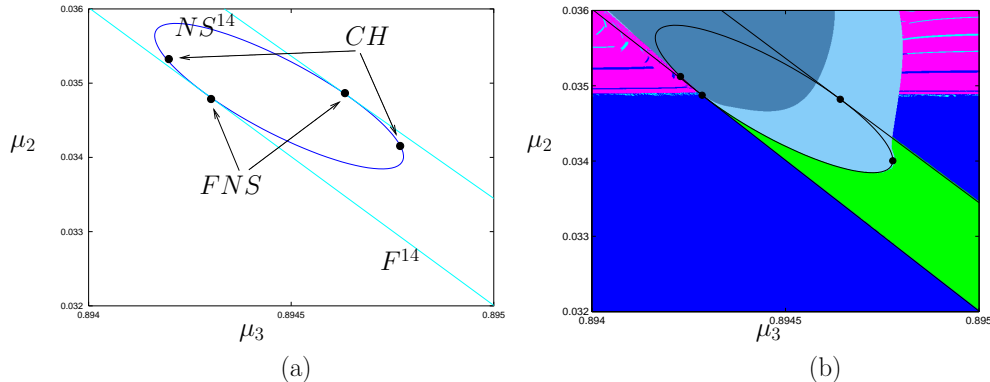


Figure 6: A subset of the bifurcation diagram near the \widetilde{CN} bifurcation set. Here codim 1 curves are labeled as in Figure 4. The codim 2 points are marked by FNS = fold-Neimark-Sacker and CH = Chenciner bifurcation.

Again at the bottom of Figure 6 there is the doubled invariant circle of focus type, phase-locked or not. Going up along the borders the 2-torus is born. This happens near $\mu_2 \approx .0348$, but the transition is not sharply visible as not only all three Lyapunov exponents are close to zero, also the amplitudes for the frequency analysis are very small, causing numerical difficulties. The stripes in this region represent 2-tori with a resonant frequency vector. If we go up in the region of resonance in \widetilde{CN} , we cross the circle of Neimark-Sacker bifurcations. There is a Chenciner point on the lower arc of the bifurcation circle, such that there is always a stable invariant curve of 14 pieces surrounding the doubled invariant curve. We conclude that the existence of the 2-torus is delimited by two bifurcation curves, where a stable and an unstable invariant curve of period 14 collide.

The bubbles in this 2-parameter plane correspond to tubes in the 3-dimensional (μ_1, μ_2, μ_3) -space. This figure agrees well with [21], and this is the situation we most frequently encountered. However, we still have a freedom to change the imaginary part of, for instance, \hat{g}_{032} . We changed it from -0.025 to 0.055 and examined the bubble near the \widetilde{CN} -boundary. In $(\Im(\hat{g}_{032}), \mu_3, \mu_2)$ -space, the circle of Neimark-Sacker bifurcations is a cylinder with four bifurcation curves on it, see Figure 7. Two rather straight lines are curves of the fold-Neimark-Sacker bifurcation, the dotted denote Chenciner bifurcations. Both straight curves intersect with one dotted curve, which corresponds to a codim 3 bifurcation, apparently a fold-Chenciner bifurcation. The role of the twist terms is to change from one two-parameter unfolding to another. We note that in a different setting a similar picture is found in [24].

After the whole discussion of bifurcations of cycles and invariant curves we now give two phase portraits near the bubbles. These show how co-existing attractors complicate the description of the unfolding.

4.2 Nonsymmetric NS-NS: A case study

We use an approach for the double NS bifurcation similar to that for the flip-NS bifurcation. The natural way to perturb the normal form 2 is to introduce relatively low-order resonances. These will be $2(\varepsilon_1 \bar{w}^{q_1-1}, 0)$ and $(0, \varepsilon_2 \bar{z}^{q_2-1})$. Now the choice $q_1 = 7, q_2 = 8$ gives the lowest orders compatible with Proposition 2.1. Then, as before, a final perturbation to break the invariance of

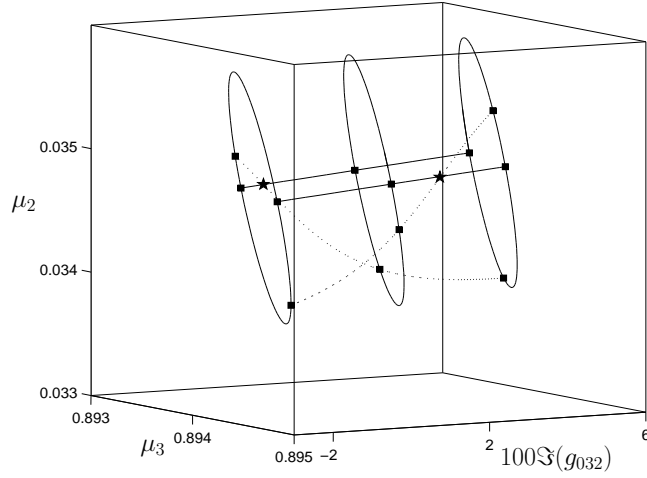


Figure 7: From one unfolding to another depending on the twist-term. The dotted lines are Chenciner bifurcation curves, which do not intersect each other. The stars indicate the position of the codim 3 bifurcations.

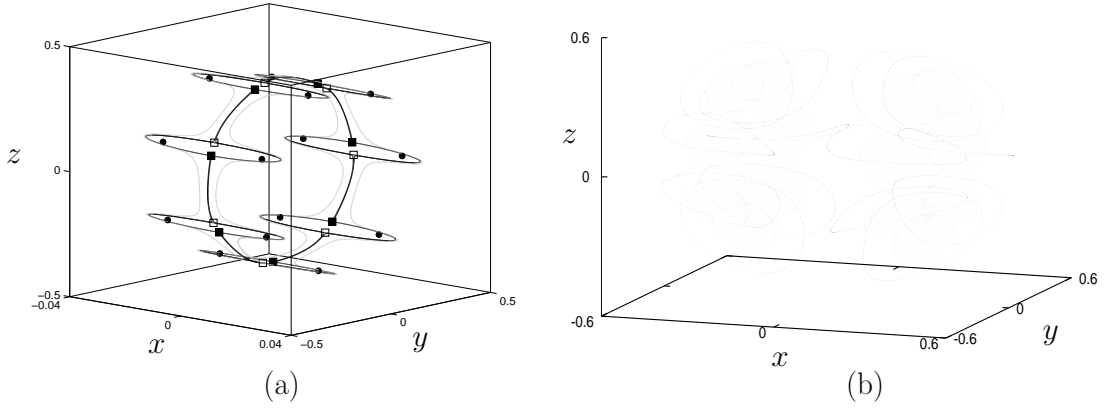


Figure 8: Phase portraits near bubbles: (a) $\mu_2 = 0.01335$, $\mu_3 = 0.9003383720148196$, \blacksquare , period-7 saddle cycle of which the 1 dimensional unstable manifold (black curve) almost reconnects to the other period-7 saddle cycle denoted by \square . Period-14 cycles are stable foci and denoted by \bullet and the grey shows the doubled invariant curve. (b) $\mu_2 = 0.0352$, $\mu_3 = 0.89479$, 2-torus surrounded by a ‘period-14’ invariant curve.

the w - and z -planes is added. The model map is now given as

$$\begin{aligned}
 F_2 : \begin{pmatrix} w \\ z \end{pmatrix} &\mapsto \begin{pmatrix} we^{i\mu_3}(1 + \mu_1) \\ ze^{i\mu_4}(1 + \mu_2) \end{pmatrix} \\
 &+ \begin{pmatrix} we^{i\mu_3} \left(\hat{f}_{2100}|w|^2 + \hat{f}_{1011}|z|^2 + \hat{f}_{3200}|w|^4 + \hat{f}_{2111}|w|^2|z|^2 + \hat{f}_{1022}|z|^4 \right) \\ ze^{i\mu_4} \left(\hat{g}_{1110}|w|^2 + \hat{g}_{0021}|z|^2 + \hat{g}_{2201}|w|^4 + \hat{g}_{1121}|w|^2|z|^2 + \hat{g}_{0032}|z|^4 \right) \end{pmatrix} \\
 &+ \begin{pmatrix} \varepsilon_1 \bar{w}^6 + \varepsilon_3 (i\Re(w)^6 + \Im(w)^6 + (1+i)(\Re(z)^6 + \Im(z)^6)) \\ \varepsilon_2 \bar{z}^7 + \varepsilon_3 ((1+2i)\Re(w)^6 + (1+i)\Im(w)^6 + \Im(z)^6) \end{pmatrix}.
 \end{aligned} \tag{8}$$

Next we choose the constants according to Table 3 and $\varepsilon_1 = 0.012i, \varepsilon_2 = 0.015, \varepsilon_3 = 0.0009$ such that also here we have the heteroclinic bifurcation.

$\hat{f}_{2100} =$	$0.03-0.03i$	$\hat{f}_{3200} =$	$0.000729-0.00018i$
$\hat{f}_{1011} =$	$0.09+0.015i$	$\hat{f}_{2111} =$	$0.000576+0.0001125i$
$\hat{g}_{1110} =$	$-0.075-0.0147i$	$\hat{f}_{1022} =$	$0.000441+0.00027i$
$\hat{g}_{2210} =$	$0.000324+0.000576i$	$\hat{g}_{1121} =$	$0.000225+0.00036i$
$\hat{g}_{0032} =$	$-0.0045-0.00018i$	$\hat{g}_{0021} =$	$-0.03+0.006i$

Table 3: Numerical values of the coefficients of map (8)

The situation is much more complicated than in the previous study, since controlling the remaining three parameters to study bifurcations of invariant objects leads to an overwhelming amount of information. However, as before, analysis of the cycles dresses the skeleton provided by the study of the amplitude map. We will restrict ourselves to the study of bifurcations of cycles and our results are much less detailed than those of the previous subsection. As before we fix the parameter $\mu_1 = -0.04$ and then increase μ_2 to control the bifurcation sequence, while we may use μ_3 and μ_4 to adjust the frequencies to the rationals.

We remark that this setup has been suggested in [38]. There, there is an thorough exploration of the dynamics on the invariant 2-tori, sketches of curves of homoclinic tangency and portraits of resonance tongues. The resonances which we study on the 2-torus display a similar organization in parameter-space.

The main structure of the tongues is given in Figure 9. If we start with μ_2 small, then there is an invariant curve, possibly phase-locked. In the lower part of the tongue there is a cycle of period 8 on the invariant curve. If we increase μ_2 , this first resonance tongue will display a bubble near the CN -bifurcation leading to a stable 2-torus. This bubble is similar to the one in the case study of the flip-NS bifurcation. There are fold-Neimark-Sacker bifurcation points, where the ellipse touches the tongue, and Chenciner points from which two invariant curves originate. These collide along two complicated sets in three-dimensional parameter space.

There is no other way to track this phenomenon but to follow a fold bifurcation curve near this set. As we introduced two resonances, we were able to locate a cycle of period 56. From the Neimark-Sacker bubble, two ellipses corresponding to fold bifurcations of the cycle of period 56 emerged. On both ellipses there are two 1:1 resonance points, which are pairwise connected by a Neimark-Sacker bifurcation curve. We have not studied the orientation of these resonance points extensively, however, we note that near the CN -bifurcation, also fold-Neimark-Sacker bifurcation points were found, which disappeared while following the period 56 cycle for bigger μ_2 . Apparently they merged with the 1:1 resonances in a triple-one bifurcation. We have not attempted to find global bifurcations, but they are certainly present.

The region where these resonances exist, seems to be a torus. Indeed, increasing μ_2 we found two swallow-tail structures on the inner-ellipse, which then transformed into a flame, i.e. a region where there are coexisting attractors of period-56, see [39, 40]. The 1:1 resonances are still present and the connecting Neimark-Sacker bifurcation curves as well.

Now let us take μ_2 near the TT -boundary, i.e. where a motion on a 3-torus may be expected, see Figure 9(c). On first sight we recognize the outer-ellipse and the inner-flame together with the 1 : 1-strong resonances. However, apart from the two Neimark-Sacker bifurcation curves similar to those in Figures 9(a) and 9(b), a third curve(dashed) is present. It touches both fold bifurcation curves and makes two loops. On the left loop it intersects one of the Neimark-Sacker bifurcation curves. Here we have a double Neimark-Sacker bifurcation. We conjecture that it appears between two codim-3 bifurcations where we have two multipliers equal to one and a complex pair of modulus one. Thus, for our choice of the coefficients, a double Neimark-Sacker bifurcation appears in the unfolding of a double Neimark-Sacker bifurcation.

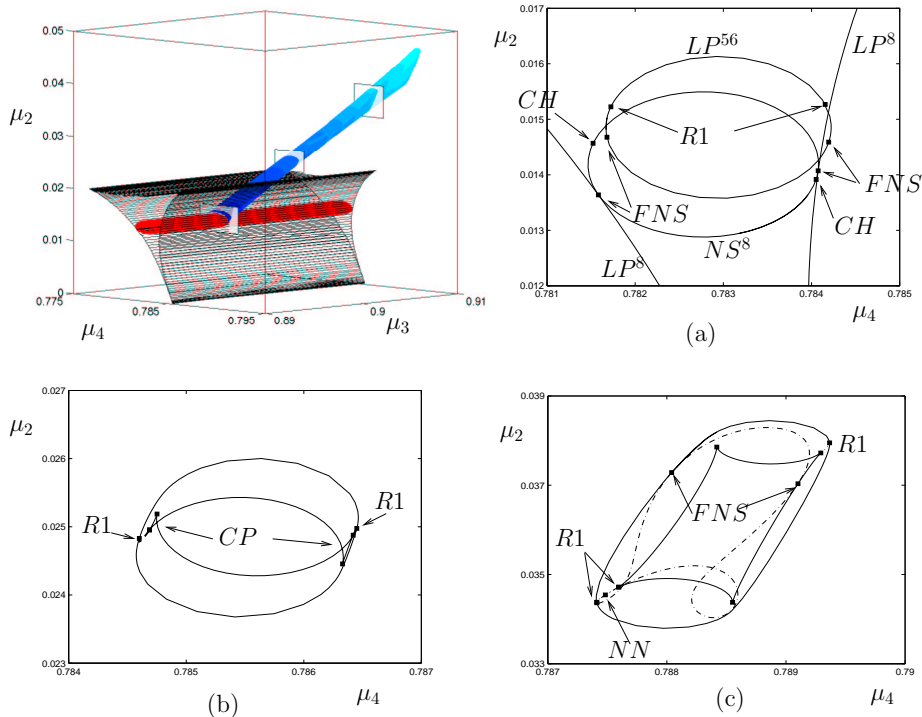


Figure 9: Bifurcation diagrams for $\mu_1 = -0.04$. The three-dimensional figures displays the period-8 tongue, the bubble inside and the emanating tube where period-56 cycles exist. The three slices correspond to the enlargements in figures (a),(b) and (c). The labels are as in the previous figures, except for CP for cusp, and NN for double Neimark-Sacker bifurcations. (a) $\mu_3 = 0.8972$; The period-8 tongue and the Neimark-Sacker bubble with Chenciner points on it, similar to that in the flip-Neimark-Sacker bifurcation. The upper ellipse are two curves of fold bifurcation of a period-56 cycle, which are indistinguishable. (b) $\mu_3 = 0.902$; The inner ellipse has developed two swallow-tails. (c) $\mu_3 = 0.9073$; An extra Neimark-Sacker bifurcation curve is present, which intersects the one that connects two R1-points at NN .

5 Center Manifold Reduction

So far we have been dealing with the normal forms and their perturbations in the minimal dimensions. To predict the bifurcation diagram of a given map in \mathbb{R}^n with a flip-NS or NS-NS bifurcation, the critical normal form coefficients on the center manifold have to be computed. For an introduction to the properties of the center manifold we refer to [28, 29]. Although it is not unique, the qualitative information does not depend on the particular selection of the center manifold. For that we employ the same technique as in [4]. Although we have not dealt with the fold-Neimark-Sacker bifurcation in this paper (see [5]), we compute its critical coefficients so that, together with [4], all codim 2 bifurcations of fixed points for maps are covered. We restrict ourselves to at most third-order terms, since this is enough to determine the unfolding except for the stability of the 2-torus for the flip-NS bifurcation or the 3-torus for the double NS bifurcation. The computations can easily be extended to include the 4th- and 5th-order terms.

Let us introduce some notations by writing the map at the critical parameter values as

$$F(u) = Au + \frac{1}{2}B(u, u) + \frac{1}{6}C(u, u, u) + \mathcal{O}(\|u\|^4), \quad u \in \mathbb{R}^n, \quad (9)$$

where $\|u\| = \sqrt{\langle u, u \rangle}$ is the standard norm in \mathbb{R}^n , $A = DF_u(0)$ and the multi-linear functions

$$B(\xi, \eta) = DF_{uu}(0)[\xi, \eta], C(\xi, \eta, \chi) = DF_{uuu}(0)[\xi, \eta, \chi].$$

Proposition 5.1 *Let F_i for $i = 1, 2, 3$ be sufficiently smooth maps, and $(k\phi \bmod 2\pi) \neq 0$ for $k = 1, 2, 3, 4$ and $(\phi_1/\phi_2) \notin \pm\{3, 2, \frac{3}{2}, 1, \frac{2}{3}, \frac{1}{2}, \frac{1}{3}\}$.*

- *Let $F_1 : \mathbb{R}^n \rightarrow \mathbb{R}^n, n \geq 3$, be a map whose fixed point at origin has only the algebraically simple multipliers $\{-1, e^{i\phi}, e^{-i\phi}\}$ on the unit circle. Then, there is a smooth local parameterization of the center manifold by $(x, z) \in \mathbb{R} \times \mathbb{C}$ such that the 5-jet of the map will assume the form (1) with the 3rd-order coefficients given by*

$$\begin{aligned} f_{300} &= \frac{1}{6}\langle p_1, C(q_1, q_1, q_1) + 3B(q_1, h_{200}) \rangle, \\ f_{111} &= \langle p_1, C(q_1, q_2, \bar{q}_2) + B(q_1, h_{011}) + 2\Re(B(q_2, h_{101})) \rangle, \\ g_{210} &= \frac{1}{2}\langle p_2, C(q_1, q_1, q_2) + B(q_2, h_{200}) + 2B(q_1, h_{110}) \rangle, \\ g_{021} &= \frac{1}{2}\langle p_2, C(q_2, q_2, \bar{q}_2) + B(q_2, h_{011}) + 2B(\bar{q}_2, h_{020}) \rangle, \end{aligned} \quad (10)$$

where

$$\begin{aligned} h_{200} &= (I_n - A)^{-1}B(q_1, q_1), \\ h_{011} &= (I_n - A)^{-1}B(q_2, \bar{q}_2), \\ h_{110} &= -(e^{i\phi}I_n + A)^{-1}B(q_1, q_2), \\ h_{020} &= (e^{2i\phi}I_n - A)^{-1}B(q_2, q_2), \end{aligned}$$

and vectors q_1, p_1, q_2, p_2 satisfy

$$\begin{aligned} Aq_1 &= -q_1, & A^T p_1 &= -p_1, & \langle p_1, q_1 \rangle &= 1, \\ Aq_2 &= e^{i\phi}q_2, & A^T p_2 &= e^{-i\phi}p_2, & \langle p_2, q_2 \rangle &= 1. \end{aligned}$$

- *Let $F_2 : \mathbb{R}^n \rightarrow \mathbb{R}^n, n \geq 3$, be a map whose fixed point at origin has only the algebraically simple multipliers $\{1, e^{i\phi}, e^{-i\phi}\}$ on the unit circle. Then, there is a smooth local parameterization of the center manifold by $(x, z) \in \mathbb{R} \times \mathbb{C}$ such that the 3-jet of the map will assume the form*

$$\begin{pmatrix} x \\ z \end{pmatrix} \mapsto \begin{pmatrix} x + f_{011}z\bar{z} + f_{200}x^2 + f_{300}x^3 + f_{111}xz\bar{z} \\ e^{i\phi}z + g_{110}xz + g_{210}zx^2 + g_{021}z^2\bar{z} \end{pmatrix}, \quad (11)$$

where

$$f_{200} = \frac{1}{2}\langle p_1, B(q_1, q_1) \rangle, \quad f_{011} = \langle p_1, B(q_2, \bar{q}_2) \rangle, \quad g_{110} = \langle p_2, B(q_1, q_2) \rangle,$$

while $f_{300}, f_{111}, g_{210}$ and g_{021} coincide with those in (10), where, however,

$$\begin{aligned} h_{200} &= (A - I_n)^{INV} (2f_{200}q_1 - B(q_1, q_1)), \\ h_{011} &= (A - I_n)^{INV} (f_{011}q_1 - B(q_2, \bar{q}_2)), \\ h_{110} &= (A - e^{i\phi}I_n)^{INV} (g_{110}q_2 - B(q_1, q_2)), \\ h_{002} &= (e^{2i\phi}I_n - A)^{-1}B(q_2, q_2), \end{aligned}$$

where h_{200} is the unique solution of $(A - I_n)h_{200} = (2f_{200}q_1 - B(q_1, q_1))$ satisfying $\langle p_1, h_{200} \rangle = 0$, and h_{011}, h_{110} are defined similarly. The vectors q_1, p_1, q_2, p_2 satisfy

$$\begin{aligned} Aq_1 &= q_1, & A^T p_1 &= p_1, & \langle p_1, q_1 \rangle &= 1, \\ Aq_2 &= e^{i\phi}q_2, & A^T p_2 &= e^{-i\phi}p_2, & \langle p_2, q_2 \rangle &= 1. \end{aligned}$$

- *Let $F_3 : \mathbb{R}^n \rightarrow \mathbb{R}^n, n \geq 4$, be a map whose fixed point at origin has only the algebraically simple multipliers $\{e^{\pm i\phi_1}, e^{\pm i\phi_2}\}$ on the unit circle. Then, there is a smooth local parameterization of the center manifold by $(w, z) \in \mathbb{C} \times \mathbb{C}$ such that the 5-jet of the map will assume the form (2) with the 3rd-order coefficients given by*

$$\begin{aligned} f_{2100} &= \frac{1}{2}\langle p_1, C(q_1, q_1, \bar{q}_1) + B(q_1, h_{1100}) + 2B(\bar{q}_1, h_{2000}) \rangle, \\ f_{1011} &= \frac{1}{2}\langle p_1, C(q_1, q_2, \bar{q}_2) + B(q_1, h_{0011}) + B(\bar{q}_2, h_{1010}) + B(q_2, h_{1001}) \rangle, \\ g_{1110} &= \frac{1}{2}\langle p_2, C(q_1, \bar{q}_1, q_2) + B(q_2, h_{1100}) + B(\bar{q}_1, h_{1010}) + B(q_1, h_{0110}) \rangle, \\ g_{0021} &= \frac{1}{2}\langle p_2, C(q_2, q_2, \bar{q}_2) + B(q_2, h_{0011}) + 2B(\bar{q}_2, h_{0020}) \rangle, \end{aligned}$$

where

$$\begin{aligned} h_{2000} &= (e^{2i\phi_1} I_n - A)^{-1} B(q_1, q_1), & h_{0020} &= (e^{2i\phi_2} I_n - A)^{-1} B(q_2, q_2), \\ h_{1100} &= (I_n - A)^{-1} B(q_1, \bar{q}_1), & h_{0011} &= (I_n - A)^{-1} B(q_2, \bar{q}_2), \\ h_{1010} &= (e^{i(\phi_1 + \phi_2)} I_n - A)^{-1} B(q_1, q_2), & h_{1001} &= (e^{i(\phi_1 - \phi_2)} I_n - A)^{-1} B(q_1, \bar{q}_2). \end{aligned}$$

h_{0110} and h_{0101} can be computed by complex conjugation, and vectors q_1, p_1, q_2, p_2 satisfy

$$\begin{aligned} Aq_1 &= e^{i\phi_1} q_1, & A^T p_1 &= e^{-i\phi_1} p_1, & \langle p_1, q_1 \rangle &= 1, \\ Aq_2 &= e^{i\phi_2} q_2, & A^T p_2 &= e^{-i\phi_2} p_2, & \langle p_2, q_2 \rangle &= 1. \end{aligned}$$

Proof. See Section 8.3. □

Remark 5.2 For the flip-Neimark-Sacker bifurcation we need to proceed with the quartic and quintic terms, only if we find $f_{300}\Re(e^{-i\phi}g_{021}) > 0$ and $f_{300}\Re(e^{-i\phi}g_{021}) - f_{111}\Re(e^{-i\phi}g_{111}) < 0$.

Remark 5.3 Remark that for the fold-Neimark-Sacker bifurcation $(A - I_n)$ is singular, but that $2f_{200}q_1 - B(q_1, q_1)$ is orthogonal to the null-space of $(A - I_n)$. Therefore the bordered nonsingular equation

$$\begin{pmatrix} A - I_n & q_1 \\ p_1^T & 0 \end{pmatrix} \begin{pmatrix} h_{200} \\ 0 \end{pmatrix} = \begin{pmatrix} 2f_{200}q_1 - B(q_1, q_1) \\ 0 \end{pmatrix}$$

yields the desired vector h_{200} . Similarly we obtain h_{011} and h_{110} .

We may further transform (11) to the hypernormalforms

$$\begin{pmatrix} x \\ z \end{pmatrix} \mapsto \begin{pmatrix} x + sz\bar{z} + x^2 + cx^3 \\ e^{i\phi}z + axz + bx^2 \end{pmatrix}, \quad (12)$$

if $f_{200}f_{011} \neq 0$ and where the coefficients for (12) are given by

$$\begin{aligned} b &= \frac{1}{f_{011}f_{200}^2} \left(f_{011}g_{102} + g_{110} \left(\frac{1}{2}f_{111} + \Re(g_{021}e^{-i\phi}) \right) - f_{200}g_{021}e^{-i\phi} \right), \\ a &= \frac{g_{011}}{f_{200}}, & c &= \frac{f_{300}}{(f_{200})^2}, & s &= \text{sign}(f_{200}f_{011}). \end{aligned}$$

6 Examples

Here we give examples of a flip-NS and a double NS bifurcation in time-periodic ODE-systems appearing in applications.

6.1 Example of flip-NS bifurcation: Control of a robot-arm.

We consider a model describing motions of a robot-arm from [31, 10]. Through two torques M_1 and M_2 the endpoint of the arm should be controlled to move on a circle. The equations of motion are

$$\begin{aligned} \begin{pmatrix} M_1 \\ M_2 \end{pmatrix} &= \begin{pmatrix} \frac{\ell}{3} + \frac{4}{3} + \cos \phi_2 & -(\frac{1}{3} + \frac{1}{2} \cos \phi_2) \\ -(\frac{1}{3} + \frac{1}{2} \cos \phi_2) & \frac{1}{3} \end{pmatrix} \begin{pmatrix} \ddot{\phi}_1 \\ \ddot{\phi}_2 \end{pmatrix} + \begin{pmatrix} k_1 \dot{\phi}_1 \\ k_2 \dot{\phi}_2 \end{pmatrix} \\ &+ \begin{pmatrix} \frac{1}{2} \dot{\phi}_2 (\dot{\phi}_2 - 2\dot{\phi}_1) \sin \phi_2 \\ \frac{1}{2} (\dot{\phi}_1)^2 \end{pmatrix} + k_G \begin{pmatrix} (\frac{\ell}{2} + 1) \cos \phi_1 + \frac{1}{2} \cos(\phi_2 - \phi_1) \\ -\frac{1}{2} \cos(\phi_2 - \phi_1) \end{pmatrix}. \end{aligned}$$

A reference solution is specified by

$$\begin{aligned} x_{spec} &= l(\cos \phi_1 + \cos(\phi_2 - \phi_1)) = L - r \cos(\omega t), \\ y_{spec} &= l(\sin \phi_1 - \sin(\phi_2 - \phi_1)) = r \sin(\omega t) \end{aligned}$$

and we want to know if it is stable under perturbations. To this end, we write $\psi_i = \phi_i - \phi_{i,spec}$ and $M_i = M_{i,spec} + \Delta M_i$ to measure deviations. To obtain stability the following control law was stipulated: $\Delta M_1 = R\psi_1$ and $\Delta M_2 = R\psi_2/3$. The above relations are inserted into the equations of motion and expanded in terms of $\psi_i, \dot{\psi}_i$ and $\ddot{\psi}_i$ for $i = 1, 2$ up to third order. The third order approximation near the origin is sufficient to characterize almost all bifurcations of codimension one and two. This yields a four dimensional vector field with periodic coefficients as functions of ϕ_1 and ϕ_2 and their derivatives. These can be expressed in terms of x_{spec} and y_{spec} . Then time was scaled such that the period is $T = 2\pi$. This affects the damping and control coefficients, see Eq. (13).

Under variation of the control parameter R and the angular velocity ω , the stability of the origin, which is always a solution of the new system, is analyzed by considering the time- T map numerically. This yielded a local bifurcation diagram with period-doubling and Neimark-Sacker bifurcations, see Figure 10.

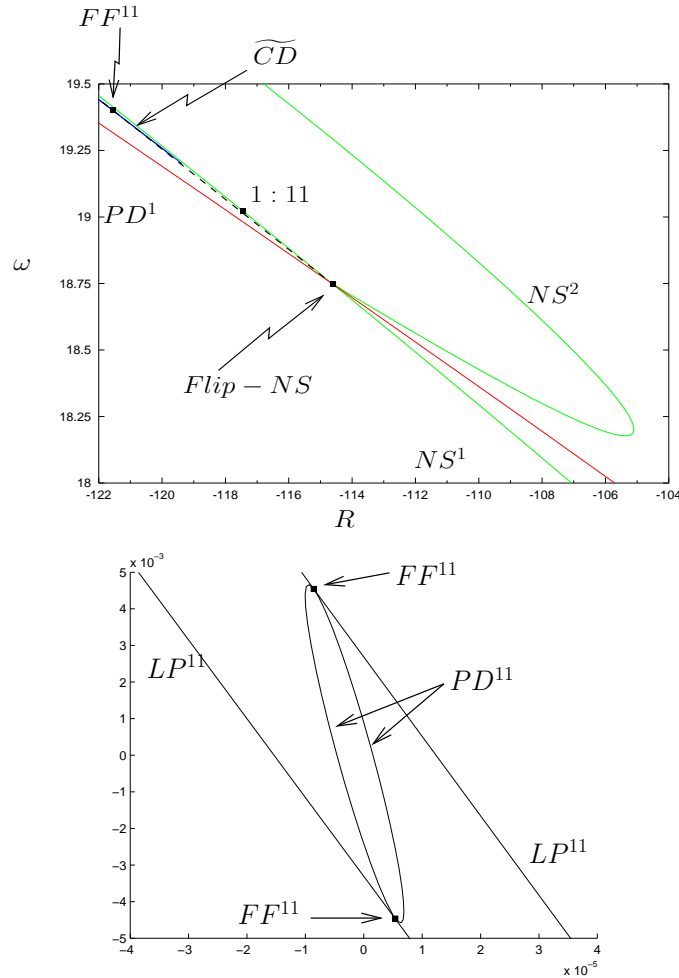


Figure 10: Local bifurcation diagram near the flip-Neimark-Sacker bifurcation. PD^1 = period doubling of the origin, NS^1 Neimark-Sacker of the origin, NS^2 = Neimark-Sacker of the period two point, \widetilde{CD} = period doubling of an invariant circle (sketch). Also displayed near \widetilde{CD} is an Arnol'd tongue of a cycle of period 11 bounded by $LP_{1,2}^{11}$. On this tongue are two fold-flip points FF^{11} , see also the rotated magnification of this piece together with the period-doubling ellipse PD^{11} . The DPD points have not been computed.

For the following parameter values a period-doubling curve and a Neimark-Sacker curve are intersecting:

$$\begin{aligned} m_1 = m_2 = 10, \rho = \frac{m_1}{m_2}, l = .4, L = .5, r = .1, \omega = 18.7468, \\ R = -\frac{114.5978}{m_2\omega^2l^2}, \quad k_1 = k_2 = \frac{0.5}{m_2\omega^2l}, \quad k_g = \frac{9.81}{\omega^2l}. \end{aligned} \quad (13)$$

Using the Runge-Kutta-Fehlberg integrator of order 7-8 combined with automatic differentiation (as in [4]), we obtained the Poincaré map with the derivatives up to third order. Thus we were able to evaluate the formulas derived in section 4.1 and 2.2 and to obtain

$$a_{11} = -12.7794, \quad a_{12} = -2.0639, \quad a_{21} = 1.4932, \quad a_{22} = -1.7381.$$

This corresponds to the “simple” case, however a stable doubled invariant circle appears nearby, see Figure 11.

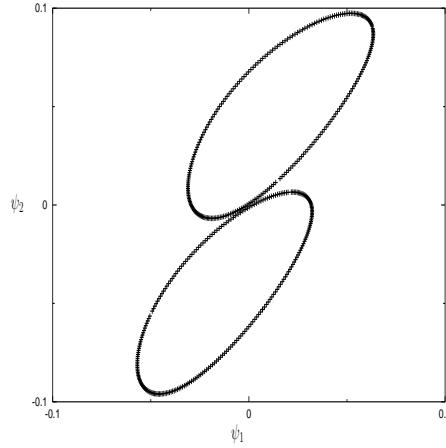


Figure 11: The stable doubled invariant curve.

6.2 Example of double NS bifurcation: Control of vibrations.

Here we consider a system of two coupled oscillating masses from [32], where one mass is used to suppress vibrations of the other. Using averaging, many details of periodic solutions are found, while here we consider the trivial solution to demonstrate the results of this article only.

The system is given by

$$\begin{cases} \ddot{x}_1 + \kappa_1(\dot{x}_1 - \dot{x}_2) + Q^2(1 + \varepsilon \cos(\eta t))(x_1 - x_2) = 0, \\ \ddot{x}_2 - M\kappa_1(\dot{x}_1 - \dot{x}_2) - MQ^2(1 + \varepsilon \cos(\eta t))(x_1 - x_2) \\ \quad + \kappa_2\dot{x}_2 + x_2 - \beta V^2(1 - \gamma\dot{x}_2^2)x_2 = 0. \end{cases}$$

The natural frequencies of this system are

$$\Omega_{1,2} = \frac{1}{2}(1 + Q^2(1 + M)) \mp \sqrt{\frac{1}{4}(1 + Q^2(1 + M))^2 - Q^2}.$$

Near the parametric resonance $\eta_0 = \Omega_2 - \Omega_1$, the trivial solution exhibits a double NS bifurcation when $k_1 = (\beta V^2 - k_2)/(1 + M) = .091666\dots$ and $\eta = 0.41101\dots$

For numerical demonstration we use the values from [32]:

$$\varepsilon = 0.1, \quad k_2 = 0.1, \quad \beta = 0.1, \quad V = \sqrt{2.1}, \quad \gamma = 4, \quad Q = 0.95, \quad M = 0.2.$$

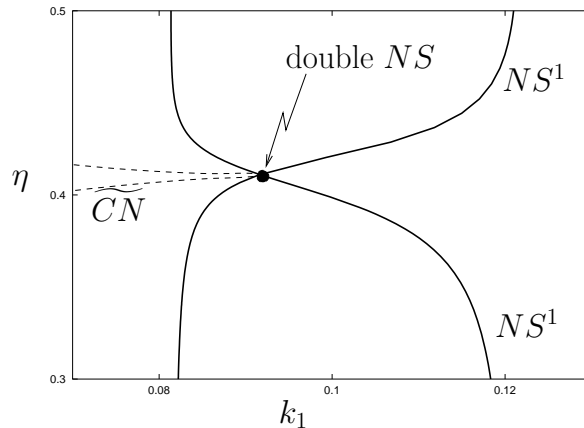


Figure 12: Local bifurcation diagram near the double Neimark-Sacker-bifurcation. $NS^1 =$ Neimark-Sacker of the origin, \widehat{CN} = transition from invariant circle to 2-torus(sketch).

As for the previous example we compute the normal form coefficients and we find

$$a_{11} = -2.0199, \quad a_{12} = -2.7841, \quad a_{21} = -0.2282, \quad a_{22} = -4.6230.$$

Now we can look up the unfolding in [2] and it is the simple case II. Taking parameters around the double NS point we have two routes from the stable trivial solution to a stable 2-torus.

Alternatively, one could have considered the averaged system. Then instead of a double NS one deals with a double Hopf bifurcation and one may apply center manifold reduction for ODE's from [2] to find a similar result.

7 Conclusions

This paper completes in some sense the analysis of local codimension two bifurcations of fixed points for maps. Together with the descriptions in [2, 5] for all cases there is now a proper analysis of the truncated normal form. Also essential critical normal form coefficients on center manifolds are available now for all cases, so that analysis of concrete maps can be performed straightforwardly. A work in progress is the implementation of these formulas into MATCONT [30].

We have combined various analytical and numerical methods to study the dynamics in the symmetric and perturbed normal forms. Although the theoretical picture already shows a richness of bifurcations, we notice that our studies indicate even further complications. Here we have focused primarily on local bifurcations, but global bifurcations are present.

There are several open problems for future research. First of all, in both the flip-Neimark-Sacker and the double Neimark-Sacker bifurcation the heteroclinic structures involve complex dynamics which is not yet well described. The resonances on the 2- and 3-tori can be mapped in more detail. Then the effect of asymmetric perturbations and the relation of the truncated normal form and the original map can be investigated in more detail. Studies in this direction have been performed in [20, 33, 34, 6, 35], but might be done even more systematically using available symbolic and numerical tools.

8 Appendix: Proofs

8.1 Section 2

Proof of Proposition 2.1. The proof proceeds in several steps. First we consider the flip-NS bifurcation and then repeat the same steps for the double NS bifurcation, where only some details are different.

Case I: Flip-NS

Step 1. Consider a map $\xi \mapsto F(\xi, \alpha)$, $\xi = (x, z) \in \mathbb{R} \times \mathbb{C}$, whose linear part at $(\xi, \alpha) = (0, 0)$ is given by

$$A = \begin{pmatrix} -1 & 0 \\ 0 & e^{i\phi} \end{pmatrix}.$$

We may apply near-identity transformations to remove as much nonresonant monomials of degree 2 and higher. Consider an elementary transformation $(x, z) \mapsto N(x, z) = (x, z)^T + (c_1, c_2)^T x^i z^j \bar{z}^k$ with $i + j + k \geq 2$ and some constants c_1, c_2 . An $x^i z^j \bar{z}^k$ -monomial can be removed from $F(\cdot, 0)$ if $\text{ad}_{A_1}(N)(x, z) := [N, A](x, z) \neq 0$, where $[\cdot, \cdot]$ is the Lie bracket operation. This leads to search of zeroes of a component of

$$\text{ad}_A(N)(x, z) = \begin{pmatrix} c_1 \left(-1 - (-1)^i e^{i\phi(j-k)} \right) \\ c_2 \left(1 - (-1)^i e^{i\phi(j-k-1)} \right) \end{pmatrix} x^i z^j \bar{z}^k, \quad 2 \leq i + j + k \leq 5.$$

Due to the absence of strong resonances, we find that $F(\xi, 0)$ may be transformed to a map with the 5-jet

$$\begin{pmatrix} x \\ z \end{pmatrix} \mapsto \begin{pmatrix} -x + f_{300}x^3 + f_{111}x|z|^2 + f_{500}x^5 + f_{311}x^3|z|^2 + f_{122}x|z|^4 \\ e^{i\phi}z + g_{210}x^2z + g_{021}z|z|^2 + g_{410}x^4z + g_{221}x^2|z|^2 + g_{032}z|z|^4 \end{pmatrix}, \quad (14)$$

where the coefficients f_{ijk} are real, while g_{ijk} are complex. The latter map coincides with NF_1 for $\alpha = 0$.

Step 2. Since 1 is not an eigenvalue of A , we may assume that the origin always is a fixed point. We write $F(\xi, \alpha) = A(\alpha)\xi + R(\xi, \alpha)$, where $R(\xi, \alpha) = \mathcal{O}(\|\xi\|^2)$. Now we introduce the parameter-dependent eigenvectors of A and A^T ,

$$A(\alpha)q_i(\alpha) = \lambda_i q_i(\alpha), \quad A^T(\alpha)p_i(\alpha) = \lambda_i p_i(\alpha), \quad (15)$$

where $\lambda_1(0) = -1$, $\lambda_2(0) = e^{i\phi}$ and $\lambda_3(0) = e^{-i\phi}$. The vectors $p_i(\alpha)$ can be scaled such that $\langle p_i(\alpha), p(\alpha)_j \rangle = \delta_{ij}$, the Kronecker delta for $i, j = 1, 2, 3$. Then the variable ξ may be written as $\xi = \eta_1 q_1(\alpha) + \eta_2 q_2(\alpha) + \bar{\eta}_2 q_3(\alpha)$, where $\bar{\eta}_2$ is treated as an independent variable. The map F , written in the η -coordinates and truncated at fifth order, takes the form

$$F(\eta, \alpha) = \begin{pmatrix} \lambda_1 \eta_1 + \sum_{2 \leq i+j+k \leq 5} f_{ijk}(\alpha) \eta_1^i \eta_2^j \bar{\eta}_2^k \\ \lambda_2 \eta_2 + \sum_{2 \leq i+j+k \leq 5} g_{ijk}(\alpha) \eta_1^i \eta_2^j \bar{\eta}_2^k \end{pmatrix}. \quad (16)$$

Now we introduce a parameter-dependent coordinate transformation $\eta = G(\xi, \alpha)$ such that $Q := j^5(F(G(\xi, \alpha), \alpha) - G(NF_1(\xi, \alpha), \alpha)) = 0$, the 5-jet w.r.t. ξ . The general form of G is

$$G(\xi, \alpha) = \begin{pmatrix} \sum_{1 \leq i+j+k \leq 5} F_{ijk}(\alpha) \xi_1^i \xi_2^j \bar{\xi}_2^k \\ \sum_{1 \leq i+j+k \leq 5} G_{ijk}(\alpha) \xi_1^i \xi_2^j \bar{\xi}_2^k \end{pmatrix},$$

where $F_{100}(0) = G_{010}(0) = 1$ and $F_{010}(0) = F_{001}(0) = G_{100}(0) = G_{001}(0) = 0$. We collect all coefficients Q_{ijk} of the monomials $\xi_1^i \xi_2^j \bar{\xi}_2^k$. Such a Q_{ijk} is a function of F_{ijk}, G_{ijk}, μ_i and the critical normal form coefficients \hat{F}_{ijk} . Thus we interpret Q as a function from $\mathbb{R}^{55} \times \mathbb{C}^{55}$ to itself. The

determinant DQ of the Jacobian matrix of Q w.r.t. F_{ijk}, G_{ijk}, μ_i and \hat{F}_{ijk} evaluated at the critical point is given by

$$DQ = \frac{-2^{51} i \sin(\phi) e^{\frac{i45\phi}{2}} \sin(\phi) \sin(3\phi) \sin(5\phi) \cos(\phi/2) (\cos(2\phi))^3 (\cos(\phi))^{10}}{(\cos(6\phi) - 1)^3 (\cos(5\phi) + 1) (\cos(4\phi) - 1)^3 (\cos(3\phi) + 1)^2 (\cos(2\phi) - 1)^{14} (\cos(\phi) + 1)^3} \quad (17)$$

Due to the non-resonance conditions imposed on ϕ , we see that $DQ \neq 0$.

Step 3. Finally we prove the regularity of the map $\tilde{G} : \alpha \mapsto \mu$. From (16) and (1) we write $\lambda_1 = -1 + \tilde{A}(\alpha)$ and $\lambda_2 = \cos(\phi) + \tilde{B}(\alpha) + i \sin(\phi) + i \tilde{C}(\alpha)$, or $|\lambda_2| = 1 + \cos(\phi) \tilde{B} + \sin(\phi) \tilde{C} + h.o.t.$. Thus we identify

$$\begin{pmatrix} \mu_1 \\ \mu_2 \end{pmatrix} = \begin{pmatrix} \tilde{A}(\alpha) \\ \cos(\phi) \tilde{B}(\alpha) + \sin(\phi) \tilde{C}(\alpha) \end{pmatrix} + h.o.t., \quad (18)$$

and we see that $\det \left(\frac{d\mu}{d\alpha} \right)_{\alpha=0} = \det \left(\frac{d(\lambda_1, |\lambda_2|)}{d\alpha} \right)_{\alpha=0} \neq 0$. Therefore we may use (1) as the unfolding for this bifurcation.

Case II: NS-NS

Step 1. Now consider a map $y \mapsto F(\xi, \alpha)$, $\xi = (w, z) \in \mathbb{C}^2$, which at $(\xi, \alpha) = (0, 0)$ has the linear part given by

$$A = \begin{pmatrix} e^{i\phi_1} & 0 \\ 0 & e^{i\phi_2} \end{pmatrix}.$$

As above we write $N(w, z) = (w, z)^T + (c_1, c_2)^T w^i \bar{w}^j z^k \bar{z}^l$ with $i + j + k + l \geq 2$ and we find

$$ad_A(N)(x, z) = \begin{pmatrix} c_1 (1 - e^{i\{\phi_1(i-j-1) + \phi_2(k-l)\}}) \\ c_2 (1 - e^{i\{\phi_1(i-j) + \phi_2(k-l-1)\}}) \end{pmatrix} w^i \bar{w}^j z^k \bar{z}^l, \quad 2 \leq i + j + k + l \leq 5.$$

Under the conditions stated we find that the map $F(\xi, 0)$ may be transformed into a map with the 5-jet

$$\begin{pmatrix} w \\ z \end{pmatrix} \mapsto \begin{pmatrix} e^{i\phi_1} w \\ e^{i\phi_2} z \end{pmatrix} + \begin{pmatrix} f_{2100} w |w|^2 + f_{1011} w |z|^2 + f_{3200} w |w|^4 + f_{2111} w |w|^2 |z|^2 + f_{1022} w |z|^4 \\ g_{1110} z |w|^2 + g_{0021} z |z|^2 + g_{2201} z |w|^4 + g_{1121} z |w|^2 |z|^2 + g_{0032} z |z|^4 \end{pmatrix}. \quad (19)$$

Remark that the coefficients f_{ijkl} and g_{ijkl} are complex.

Step 2. For the double Neimark-Sacker bifurcation a similar preparation but with two complex variables leads to a function $Q : \mathbb{C}^{250} \rightarrow \mathbb{C}^{250}$. The Jacobian DQ at the critical point is the product of expressions like $(\cos(3\phi_1 - \phi_2) - 1)^4$ and $(\cos(\phi_1 + 5\phi_2) - 1)$, but too lengthy to display here. From the non-resonance conditions required we obtain that $DQ \neq 0$ and that these are the minimal set of such conditions.

Step 3. As before we write $\lambda_1(\alpha) = \cos(\phi_1) + \tilde{A}(\alpha) + i \sin(\phi_1) + i \tilde{B}(\alpha)$ and $\lambda_2(\alpha) = \cos(\phi_2) + \tilde{C}(\alpha) + i \sin(\phi_2) + i \tilde{D}(\alpha)$ and at first order the map $\tilde{G} : \alpha \mapsto \mu$ is given as

$$\begin{pmatrix} \mu_1 \\ \mu_2 \end{pmatrix} = \begin{pmatrix} \cos(\phi_1) \tilde{A}(\alpha) + \sin(\phi_1) \tilde{B}(\alpha) \\ \cos(\phi_2) \tilde{C}(\alpha) + \sin(\phi_2) \tilde{D}(\alpha) \end{pmatrix} + h.o.t., \quad (20)$$

The map regularity of $\tilde{G} : \alpha \mapsto \mu$ at 0 is now ensured by $|D_\alpha(\mu)|_{\alpha=0} = |D_\alpha(|\lambda|)|_{\alpha=0} \neq 0$. \square

Computations for Remark 2.2. It is sufficient to verify the statement for the normal forms, so DG_i should be nonzero. A straightforward calculation shows that

$$\det DG_1(0, 0) = 16 \sin^2(\phi) \left| \frac{d(\lambda_1, \lambda_2)}{d(\alpha_1, \alpha_2)} \right|.$$

For the regularity of G_2 we use DF_2 as in the beginning of Section 2 and introduce $B^T = C = \begin{pmatrix} 1 & 0 & 0 & 0 & 0 & 0 \\ 0 & 0 & 0 & 0 & 0 & 1 \end{pmatrix}$. Then indeed the 8×8 -matrix in the Remark is nonsingular. After some tedious algebra one finds

$$\frac{d(g_{11}, g_{22})}{d(\alpha_1, \alpha_2)} = \begin{pmatrix} \frac{\partial(\cos(\phi_1)\tilde{A} + \sin(\phi_1)\tilde{B})}{\partial\alpha_1} & \frac{\partial(\cos(\phi_1)\tilde{A} + \sin(\phi_1)\tilde{B})}{\partial\alpha_2} \\ \frac{\partial(\cos(\phi_2)\tilde{C} + \sin(\phi_2)\tilde{D})}{\partial\alpha_1} & \frac{\partial(\cos(\phi_2)\tilde{C} + \sin(\phi_2)\tilde{D})}{\partial\alpha_2} \end{pmatrix}.$$

In fact we have $\det DG_2(0, 0) = 16(\cos(\phi_1) - 1)(\cos(\phi_2) - 1) \left| \frac{d(|\lambda_1|, |\lambda_2|)}{d(\alpha_1, \alpha_2)} \right|$. \square

Proof of Proposition 2.3. We introduce a special change of coordinates M consisting of the resonant monomials in the 3-jet of (3). The transformation leads to a new map F with the same 3-jet but alters the 5-jet. Then we choose the $m_i, i = 1, 2, 3, 4$ such that as many as possible of the $c_i, i = 1, 2, \dots, 6$ are eliminated. We write

$$\begin{aligned} M(x, y) &= \begin{pmatrix} x + m_1x^3 + m_2xy^2 \\ y + m_3x^2y + m_4y^3 \end{pmatrix}, \\ F(x, y) &= \begin{pmatrix} x + a_{11}x^3 + a_{12}xy^2 + c_1x^5 + c_2x^3y^2 + c_3xy^4 \\ y + a_{21}x^2y + a_{22}y^3 + c_4x^4y + c_5x^2y^3 + c_6y^5 \end{pmatrix}. \end{aligned}$$

The condition $j^5(H(M(x, y)) - M(F(x, y))) = 0$ leads to the following linear system in the m_i

$$2 \begin{pmatrix} a_{12} & a_{21} - a_{11} & -a_{12} & 0 \\ 0 & a_{22} & 0 & -a_{12} \\ -a_{21} & 0 & a_{11} & 0 \\ 0 & -a_{21} & a_{12} - a_{22} & a_{21} \end{pmatrix} \begin{pmatrix} m_1 \\ m_2 \\ m_3 \\ m_4 \end{pmatrix} = \begin{pmatrix} h_{32} - c_2 \\ h_{14} - c_3 \\ h_{41} - c_4 \\ h_{23} - c_5 \end{pmatrix}. \quad (21)$$

Note that the coefficients of x^5 - and y^5 -terms are not affected by this transformation. The matrix has determinant zero and its kernel has dimension 1. Therefore we can select only three terms to be removed out of six fifth-order terms. If we choose not to kill c_4 , then this coincides with a natural nondegeneracy condition in the bifurcation analysis. Thus we set $c_2 = c_3 = c_5 = m_3 = 0$ and solve equation (21) in m_1, m_2, m_4 and c_1, c_4, c_6 . We get the new coefficients

$$c_1 = h_{50}, \quad c_6 = h_{05}, \quad c_4 = h_{41} + a_{21} \left(\frac{h_{32}}{a_{12}} - \frac{h_{14}(a_{11} - a_{21})}{a_{12}(a_{12} - a_{22})} - \frac{h_{23}(a_{11} - a_{21})}{a_{21}(a_{12} - a_{22})} \right).$$

Then we apply a linear scaling $x \rightarrow x/\sqrt{|a_{11}|}, y \rightarrow y/\sqrt{|a_{22}|}$ and obtain the desired map. \square

8.2 Section 3

Proof of Proposition 3.1

1. The fixed point equation is given by $x = (1 + \mu_1)x + s_1x^3 + c_1x^5$. For μ_1 small we have $x_+ = \sqrt{-\mu_1 s_1} + \mathcal{O}(\mu_1)$. The extra fixed point exists for $\mu_1 s_1 < 0$. We evaluate the Jacobian

$$\begin{aligned} DF_\mu(x_+, 0) &= \begin{pmatrix} 1 + \mu_1 + 3s_1x_+^2 + 5c_1x_+^4 & 0 \\ 0 & 1 + \mu_2 + s_1\delta x_+^2 + c_4x_+^4 \end{pmatrix} \\ &= \begin{pmatrix} 1 - 2\mu_1 + \mathcal{O}(\mu_1^2) & 0 \\ 0 & 1 + \mu_2 - \delta\mu_1 + \mathcal{O}(\mu_1^2) \end{pmatrix}. \end{aligned}$$

The multiplier in the x -direction is $\mu_{\hat{x}} = 1 - 2\mu_1 + \mathcal{O}(\mu_1^2)$, so in this direction it is stable if $s_1 < 0$ and unstable if $s_1 > 0$. In the y -direction it is stable if $\mu_2 - \delta\mu_1 < 0$.

2. This is analogous to the preceding item.

3. For a nontrivial fixed point we search for nonzero (x, y) with

$$\begin{pmatrix} s_1 & s_2\theta \\ s_1\delta & s_2 \end{pmatrix} \begin{pmatrix} x^2 \\ y^2 \end{pmatrix} = - \begin{pmatrix} \mu_1 \\ \mu_2 \end{pmatrix} + \begin{pmatrix} c_1x^4 \\ c_4x^4 + c_6y^4 \end{pmatrix}.$$

A solution is $(x^2, y^2) = (\rho_1^2, \rho_2^2) = \frac{1}{s_1s_2(\delta\theta-1)}(s_2(\mu_1 - \theta\mu_2), s_1(\mu_2 - \delta\mu_1)) + \mathcal{O}(\|\mu\|^2)$. It exists if both components are positive. Now we turn to the stability of this point. From the Routh-Hurwitz criterion it follows that the roots of $\lambda^2 + a_1\lambda + a_0 = 0$ are strictly inside the unit circle if and only if

$$|a_1| < (1 + a_0), \quad (22a)$$

$$|a_0| < 1. \quad (22b)$$

We give the Taylor expansions in μ of the trace and determinant:

$$\begin{aligned} a_1 = \text{tr}(DF_\mu(\rho_1, \rho_2)) &= 2 - \frac{2}{\delta\theta - 1}((\delta - 1)\mu_1 + (\theta - 1)\mu_2) \\ &\quad + z_{20}\mu_1^2 + z_{11}\mu_1\mu_2 + z_{02}\mu_2^2 + \mathcal{O}(\|\mu\|^2), \\ a_0 = \det(DF_\mu(\rho_1, \rho_2)) &= 1 - \frac{2}{\delta\theta - 1}((\delta - 1)\mu_1 + (\theta - 1)\mu_2) \\ &\quad + \hat{z}_{20}\mu_1^2 + \hat{z}_{11}\mu_1\mu_2 + \hat{z}_{02}\mu_2^2 + \mathcal{O}(\|\mu\|^2), \end{aligned}$$

where

$$z_{20} - \hat{z}_{20} = \frac{-4\delta}{\delta\theta - 1}, z_{11} - \hat{z}_{11} = \frac{4(\delta\theta + 1)}{\delta\theta - 1}, z_{02} - \hat{z}_{02} = \frac{-4\theta}{\delta\theta - 1}.$$

A little algebra shows that conditions (22a) and (22b) are equivalent to

$$\frac{4}{\delta\theta - 1}(\delta\mu_1 - \mu_2)(\theta\mu_2 - \mu_1) = 4s_1s_2(\delta\theta - 1)\rho_1^2\rho_2^2 < 0 + \mathcal{O}(\|\mu\|^2), \quad (23a)$$

$$-\frac{2}{\delta\theta - 1}((\theta\mu_2 - \mu_1) + (\delta\mu_1 - \mu_2)) = 2(s_1\rho_1^2 + s_2\rho_2^2) < 0 + \mathcal{O}(\|\mu\|^2), \quad (23b)$$

if μ is sufficiently small.

4. Violation of (22b) corresponds to a Neimark-Sacker bifurcation of the nontrivial fixed point. This can only occur if $s_1s_2 < 0$. Consider now μ_1 as a perturbation parameter, then a first order approximation for the critical value is given by $\mu_{2,c} = -(\delta - 1)\mu_1/(\theta - 1)$. Now the first order approximation of the multiplier is $\lambda = 1 + 2\mu_1\sqrt{(1 - \delta\theta)/(\theta - 1)}$, which is complex if $\delta\theta > 1$. For sufficiently small μ_1 we are not near strong resonances. Then we used one more order in the approximations of x, y, μ_2, λ and the (adjoint) eigenvectors p, q of the Jacobi matrix along the bifurcation curve. Then we verified transversality $\frac{d|\lambda|}{d\mu_2}|_{\mu_2=\mu_{2,c}} = \frac{1}{2}$, and for the nondegeneracy we computed the leading term of the Lyapunov coefficient L_{NS} and found

$$\begin{aligned} L_{NS} &= \Re(\bar{\lambda}\langle p, C(q, q, \bar{q}) \\ &\quad + 2B(q, (I_n - A)^{-1}B(q, \bar{q})) + B(\bar{q}, (\lambda^2 I_n - A)^{-1}B(q, q)) \rangle) \\ &= \mu_1s_1 \left(\frac{12(2\delta\theta - \delta - \theta)}{\theta(\theta - 1)} + c_1 \frac{8(2\delta\theta - \delta - 1)}{(\theta - 1)(\delta\theta - 1)} - c_4 \frac{8}{(\delta\theta - 1)} + c_6 \frac{8\delta(2\delta\theta - \theta - 1)}{\theta(\theta - 1)(\delta\theta - 1)} \right) \\ &\quad + \mathcal{O}(\mu_1^2). \end{aligned}$$

If $L_{NS} \neq 0$ a closed invariant curve appears, which is stable if L_{NS} is negative and unstable if L_{NS} is positive.

5. First we compute a vector field, whose time-1 map approximates the map (6) as in [3]. Then after a singular rescaling of the vector field we use the Pontryagin-Melnikov method. The three steps in our calculation closely follow the presentation in [37].

Step 1. If we perform Picard iterations as in for example [3], then we find that the following vector field contains all relevant terms.

$$\begin{pmatrix} \dot{x} \\ \dot{y} \end{pmatrix} = \begin{pmatrix} x(\mu_1 - \frac{1}{2}\mu_1^2 + \tilde{a}_{11}x^2 + \tilde{a}_{12}y^2 + \tilde{c}_1x^4 + \tilde{c}_2x^2y^2 + \tilde{c}_3y^4) \\ y(\mu_2 - \frac{1}{2}\mu_2^2 + \tilde{a}_{21}x^2 + \tilde{a}_{22}y^2 + \tilde{c}_4x^4 + \tilde{c}_5x^2y^2 + \tilde{c}_6y^4) \end{pmatrix},$$

where $\tilde{a}_{ij}, \tilde{c}_i$ are functions of c_i and a_{ij} of map (6). After applying the scaling $(x, y) \rightarrow (x/\sqrt{1-2\mu_1}, y/\sqrt{1-2\mu_2})$, these coefficients are given as

$$\begin{aligned} \tilde{a}_{11} &= s_1, & \tilde{a}_{12} &= -s_1\theta(1 - \mu_1 + \mu_2), \\ \tilde{a}_{21} &= s_1\delta(1 + \mu_1 - \mu_2), & \tilde{a}_{22} &= -s_1, \\ \tilde{c}_1 &= c_1 - \frac{3}{2}, & \tilde{c}_4 &= c_4 - \delta(1 + \frac{1}{2}\delta), \\ \tilde{c}_2 &= \theta(\delta + 2), & \tilde{c}_5 &= \delta(\theta + 2), \\ \tilde{c}_3 &= -\theta(1 + \frac{1}{2}\theta), & \tilde{c}_6 &= c_6 - \frac{3}{2} \end{aligned} \quad (24)$$

Step 2. We make a change of variables and perform a singular rescaling

$$(t, x^2, y^2, \mu_1, \mu_2) \mapsto \left(\frac{1}{2}\varepsilon^{-1}x^p y^q t, \varepsilon x, \varepsilon y, -s_1\varepsilon, \left(\frac{\delta-1}{\theta-1} \right) s_1\varepsilon + \varepsilon^2\nu \right),$$

which results in the following vector field

$$\begin{pmatrix} \dot{x} \\ \dot{y} \end{pmatrix} = s_1 x^{p-1} y^{q-1} \begin{pmatrix} x(-1 + x - \theta y), \\ y \left(\frac{\delta-1}{\theta-1} + \delta x - y \right) \end{pmatrix} + \varepsilon x^{p-1} y^{q-1} \begin{pmatrix} g_1(x, y) \\ g_2(x, y) \end{pmatrix} + \mathcal{O}(\varepsilon^2), \quad (25)$$

where

$$\begin{aligned} g_1(x, y) &= x \left(-\frac{1}{2} - y\theta \left(\frac{\delta+\theta-2}{\theta-1} \right) + \tilde{c}_1x^2 + \tilde{c}_2xy + \tilde{c}_3y^2 \right), \\ g_2(x, y) &= y \left(\nu - \frac{1}{2} \left(\frac{\delta-1}{\theta-1} \right)^2 - x\delta \left(\frac{\delta+\theta-2}{\theta-1} \right) + \tilde{c}_4x^2 + \tilde{c}_5xy + \tilde{c}_6y^2 \right). \end{aligned}$$

For $\varepsilon = 0$ this is a Hamiltonian system with

$$H(x, y) = s_1 x^p y^q (\delta\theta - 1) \left(\frac{1-x}{\theta-1} - \frac{y}{\delta-1} \right), \quad p = -\frac{(\delta-1)}{\delta\theta-1}, \quad q = -\frac{(\theta-1)}{\delta\theta-1}.$$

Step 3. We have $p, q > 0$ due to the non-degeneracy conditions. Now we treat the term proportional to ε in (25) as a small perturbation of the Hamiltonian system. We should therefore evaluate the Pontryagin-Melnikov function (see [36]) for the critical level set $H = 0$, which consists of three heteroclinic orbits.

$$\Delta(h, \nu) = \oint_{\Gamma_h} dH(s(\tau), \nu) \wedge g(s(\tau), \nu) d\tau,$$

where $s(\tau)$ corresponds to a nontrivial heteroclinic solution in the positive quadrant of the Hamiltonian system on the level curve $H = h$. Then the equation $\Delta(0, \nu) = 0$ defines a quadratic approximation to a curve on which the heteroclinic connection ‘‘survives’’ in (25) for small $\varepsilon \neq 0$.

$$\begin{aligned} \Delta(0, \nu) &= \oint_{\Gamma_0} g_1(x, y) dy - g_2(x, y) dx \\ &= \oint_{\Gamma_0} x^p y^{q-1} \left(-\frac{1}{2} - y\theta \left(\frac{\delta+\theta-2}{\theta-1} \right) + \tilde{c}_1x^2 + \tilde{c}_2xy + \tilde{c}_3y^2 \right) dy \\ &\quad - x^{p-1} y^q \left(\nu - \frac{1}{2} \left(\frac{\delta-1}{\theta-1} \right)^2 - x\delta \left(\frac{\delta+\theta-2}{\theta-1} \right) + \tilde{c}_4x^2 + \tilde{c}_5xy + \tilde{c}_6y^2 \right) dx \\ &= -I_{(p-1, q)} \left(\nu - \frac{p}{2q} - \frac{(\delta-1)^2}{2(\theta-1)^2} \right) + I_{(p, q)} \left(\frac{\delta(\theta+\delta-2)}{\theta-1} \right) \\ &\quad + I_{(p-1, q+1)} \left(\frac{\theta p(\theta+\delta-2)}{(q+1)(\theta-1)} \right) - I_{(p+1, q)} \left(\tilde{c}_4 + \frac{p+2}{q} \tilde{c}_1 \right) \\ &\quad - I_{(p, q+1)} \left(\tilde{c}_5 + \frac{p+1}{q+1} \tilde{c}_2 \right) - I_{(p-1, q+2)} \left(\tilde{c}_6 + \frac{p}{q+2} \tilde{c}_3 \right), \end{aligned} \quad (26)$$

where Green's formula is used and we defined $I_{(i,j)} = \int_{\Gamma_0} x^i y^j dx$. On the critical level curve we have $y = \frac{\delta-1}{\theta-1}(1-x)$ and with this substitution we find

$$I_{i,j} = \left(\frac{\delta-1}{\theta-1}\right)^j \int_0^1 x^i (1-x)^j dx = \left(\frac{\delta-1}{\theta-1}\right)^j \frac{\Gamma(1+i)\Gamma(1+j)}{\Gamma(2+i+j)}. \quad (27)$$

Using the definition of the Γ -function and substituting the \tilde{c}_i we can now find ν from (26)

$$\nu = \frac{(\delta\theta-1)^2}{2(\theta-1)^3} + c_1 \left(\frac{\delta(2\delta\theta-\delta-1)}{(2\delta\theta-\theta-\delta)(\theta-1)}\right) + c_4 \left(\frac{\delta}{(2\delta\theta-\theta-\delta)}\right) - c_6 \left(\frac{\theta(2\delta\theta-\theta-1)(\delta+1)^2}{(2\delta\theta-\theta-\delta)(\theta-1)^3}\right).$$

Since the time-1 flow approximates the map (6) up to order 2 in μ , this calculation shows that the curve

$$\mu_2 = -\frac{\delta-1}{\theta-1}\mu_1 + \nu\mu_1^2 + \mathcal{O}(\mu_1^3), \quad (28)$$

is an approximation of the heteroclinic connection in the map (6).

Remark 8.1 The following vector field corresponds to the truncated amplitude system for the double Hopf bifurcation for vector fields:

$$\begin{pmatrix} \dot{x} \\ \dot{y} \end{pmatrix} = \begin{pmatrix} x(\mu_1 + x^2 - \theta y^2 + \Theta y^4) \\ y(\mu_2 + \delta x^2 - y^2 + \Delta x^4) \end{pmatrix}.$$

An analogous computation shows that

$$\mu_2 = -\frac{\delta-1}{\theta-1}\mu_1 + \frac{(\theta-1)^3\delta\Delta + (\delta-1)^3\theta\Theta}{(2\delta\theta-\theta-\delta)(\theta-1)^2}\mu_1^2 + \mathcal{O}(\mu_1^3) \quad (29)$$

is the approximation of the heteroclinic bifurcation curve for this vector field. Thus the μ_1^2 -term given in [2] needs correction. In [37] a different scaling is used, but the final result is wrong as well.

8.3 Section 5

Proof of Proposition 5.1 The truncated critical normal form (11) is given by [5]. As in [3] and [4], select a parameterization $u = H(w) = \sum_{|\nu| \geq 1} \frac{1}{\nu!} h_\nu w^\nu$ of the critical center manifold such that the 3-jet of the restriction of (9) to this manifold is put in the corresponding Poincaré normal form. Then, the invariance of the center manifold allows one to find recursively all h_ν , as well as the coefficients of the critical normal form, from appearing linear systems and their Fredholm solvability conditions. \square

References

- [1] Arnol'd, V.I., Afraimovich, V.S., Il'yashenko, Yu.S. and Shil'nikov, L.P., 1994, Bifurcation theory, in: Arnol'd, V.I. (Ed): *Dynamical Systems V. Encyclopaedia of Mathematical Sciences*, New York, Springer-Verlag.
- [2] Kuznetsov, Yu.A., 2005, *Elements of Applied Bifurcation Theory*, (3rd edn), Berlin, Springer-Verlag.
- [3] Kuznetsov, Yu.A., Meijer, H.G.E. and van Veen, L., 2004, The fold-flip bifurcation, *Int. J. Bif. Chaos*, **14**, 2253–2282.
- [4] Kuznetsov, Yu.A. and Meijer, H.G.E., 2005, Numerical normal forms for codim 2 bifurcations of maps with at most two critical eigenvalues, *SIAM J. Sci. Comput.*, **26**, 1932–1954.

- [5] Broer, H.W., Simó, C. and Vitolo, R., 2004, The Hopf-Saddle-Node bifurcation for fixed points of 3D-diffeomorphisms, a dynamical inventory, preprint, University of Groningen, Netherlands.
- [6] Broer, H.W., Simó, C. and Vitolo, R., 2004, The Hopf-Saddle-Node bifurcation for fixed points of 3D-diffeomorphisms, analysis of a resonance ‘bubble’, preprint, University of Groningen, Netherlands.
- [7] Iooss, G. and Los, J.E., 1988, Quasi-genericity of bifurcations to high-dimensional invariant tori for maps, *Comm. Math. Phys.*, **119**, 453–500.
- [8] Los, J.E., 1988, Small divisor phenomena in an invariant curve doubling bifurcation on a cylinder, *Ann. Inst. H. Poincaré’ Anal. Non Linéaire*, **5**, 37–95.
- [9] Los, J.E., 1989, Non-normally hyperbolic invariant curves for maps in \mathbb{R}^3 and doubling bifurcation, *Nonlinearity*, **2**, 149–174.
- [10] Steindl, A., 1990, Bifurcation of codimension 2 for a discrete map, In: Roose, D., De Dier, B. and Spence A. (Eds) *Continuation and bifurcations: numerical techniques and applications (Leuven, 1989)*, *NATO Adv. Sci. Inst. Ser. C Math. Phys. Sci.*, **313**, 389–396, Dordrecht, Kluwer Acad. Publ..
- [11] Wen, G.-L. and Xu, D., 2004, Implicit criteria of eigenvalue assignment and transversality of bifurcation control in four-dimensional maps, *Int. J. Bif. Chaos*, **14**, 3489-3503.
- [12] Wen, G.-L. and Xu, D., 2004, Feedback control of Hopf-Hopf interaction bifurcation with development of torus solutions in high-dimensional maps, *Phys. Let. A*, **321**, 24–33.
- [13] Ding, W., Xie, J. and Sun Q., 2004, Interaction of Hopf and period doubling bifurcations of a vibro-impact system., *J. of Sound and Vibration*, **275**, 27–45.
- [14] Xie, J. and Ding, W., 2005, Hopf-Hopf bifurcation and invariant torus T^2 of a vibro-impact system., *Int. J. Non-Lin. Mech.*, **40**, 531–543.
- [15] Kuznetsov, Yu.A. and Levitin, V.V., 1995–1997, CONTENT: A multiplatform environment for analyzing dynamical systems, Dynamical Systems Laboratory, CWI, Amsterdam, Available online at: <ftp.cwi.nl/pub/CONTENT>
- [16] Govaerts, W.F.J., 2000, Numerical Methods for Bifurcations of Dynamical Equilibria, Philadelphia, SIAM.
- [17] Broer, H.W., Huitema, G.B., Takens, F. and Braaksma B.L.J., 1990, Unfoldings and bifurcations of quasi-periodic tori, *Mem. Amer. Math. Soc.*, **421**, Providence: AMS.
- [18] Chenciner, A., 1985, Bifurcations de points fixes elliptiques. I. Courbes invariantes., *Inst. Hautes E’tudes Sci. Publ. Math.*, **61**, 67–127.
- [19] Chenciner, A., 1985, Bifurcations de points fixes elliptiques. II. Orbites periodiques et ensembles de Cantor invariants., *Inst. Hautes E’tudes Sci. Publ. Math.*, **80**, 81–106.
- [20] Chenciner, A., 1988, Bifurcations de points fixes elliptiques. III. Orbites pe’riodiques de ‘petites’ periodes et élimination résonnante des couples de courbes invariantes, *Inst. Hautes E’tudes Sci. Publ. Math.*, **66**, 5–91.
- [21] Takens F. and Wagener, F.O.O, 2000, Resonances in skew and reducible quasi-periodic Hopf bifurcations, *Nonlinearity*, **13**, 377-396.
- [22] Arnol’d, V.I., 1983, Geometrical Methods in the Theory of Ordinary Differential Equations, New-York, Springer-Verlag.

- [23] Krauskopf, B. and Oldeman, B.E., 2004, A planar model system for the saddle-node Hopf bifurcation with global reinjection, *Nonlinearity*, **17**, 1119–1151.
- [24] Saleh, K., 2005, organising centres in the semi-global analysis of dynamical systems, PhD thesis, University of Groningen, Netherlands.
- [25] Borland, M., Emery, L., Hang, H. and Soliday, R., 2005, User's guide for sdds toolkit version 1.30, available online at : <http://www.aps.anl.gov/asd/oag/software.shtml>.
- [26] Cincotta, P.M., Giordano, C.M. and Simó, C., 2003, Phase space structure of multi-dimensional systems by means of the mean exponential growth factor of nearby orbits, *Phys. D*, **182**, 151–178.
- [27] Laskar, J. and Froeschle, C. and Celletti, A., 1992, The measure of chaos by the numerical analysis of the fundamental frequencies. Application to the standard mapping, *Phys. D*, **56**, 253–269.
- [28] Vanderbauwhede, A., 1988, Center manifolds and their basic properties. An introduction, In: Delft Progress Report 1, **12**, 57–78.
- [29] Vanderbauwhede, A., 1989, Centre manifolds, normal forms and elementary bifurcations, In: Dynamics reported, Vol. 2, pp. 89-169. Chichester, Wiley.
- [30] Ghaziani, R.K., Govaerts, W., Kuznetsov, Yu.A. and Meijer, H.G.E., 2006, Bifurcation analysis of periodic orbits of maps in MATLAB, in preparation.
- [31] Lindtner, E., Steindl, A. and Troger, H., 1989, Generic one-parameter bifurcations in the motion of a simple robot, *J. Comput. Appl. Math.*, **26**, 199-218.
- [32] Fatimah, S. and Verhulst, F., 2003, Suppressing flow-induced vibration by parametric excitation, *Nonlinear Dynam.*, **31**, 275–297.
- [33] Arrowsmith, D.K., Cartwright, J.H.E., Lansbury, A.N. and Place, C.M., 1993, The Bogdanov map: bifurcations, mode locking, and chaos in a dissipative system, *Int. J. Bif. Chaos*, **3**, 803-842.
- [34] Agliari, A., Bischi, G.-I., Dieci, R. and Gardini, L., 2005, Global bifurcations of closed invariant curves in two-dimensional maps: a computer assisted study, *Int. J. Bif. Chaos*, **15**, 1285–1328.
- [35] Aronson, D.G., Chory, M.A., Hall, G.R. and McGehee, R.P., 1982, Bifurcations from an invariant circle for two-parameter families of maps of the plane: A computer-assisted study, *Comm. Math. Phys.*, **83**, 303–354.
- [36] Sanders, J.A. and Verhulst, F., 1985, Averaging Methods in Nonlinear Dynamical Systems, New-York, Springer-Verlag.
- [37] Chow, Sh.-N., Li, C. and Wang, D., 1994, Normal Forms and Bifurcation of Planar Vector Fields, Cambridge University Press.
- [38] Baesens, C., Guckenheimer, J., Kim, S. and Mackay R.S., 1991, Three couples oscillators: mode-locking, global bifurcations and toroidal chaos, *Phys. D*, **49**, 387–475.
- [39] Peckham, B. B. and Kevrekidis, I.G., 2002, Lighting Arnold flames: resonance in doubly forced periodic oscillators. *Nonlinearity*, **15**, 405–428.
- [40] Broer, H.W., Golubitsky, M. and Vegter, G., 2003, The geometry of resonance tongues: a singularity theory approach. *Nonlinearity*, **16**, 1511–1538.